Institutionen för systemteknik
Department of Electrical Engineering

Examensarbete

A Method for Estimating Soot Load in a DPF Using an RF-based Sensor

Examensarbete utfört i Fordonssystem
vid Tekniska högskolan vid Linköpings universitet
av

John Hansson och Victor Ingeström

LiTH-ISY-EX--12/4584--SE

Linköping 2012

Linköpings universitet

TEKNISKA HÖGSKOLAN

Department of Electrical Engineering   Linköpings tekniska högskola
Linköpings universitet   Linköpings universitet
SE-581 83 Linköping, Sweden   581 83 Linköping

A Method for Estimating Soot Load in a DPF Using an RF-based Sensor

Examensarbete utfört i Fordonssystem
vid Tekniska högskolan i Linköping
av

John Hansson och Victor Ingeström

LiTH-ISY-EX--12/4584--SE

Handledare: **Daniel Eriksson**
    ISY, Linköpings Universitet
  Oskar Leufven
    ISY, Linköpings Universitet
  Anna Hägg
    Volvo Cars

Examinator: **Lars Eriksson**
    ISY, Linköpings universitet

Linköping, 11 June, 2012

	Avdelning, Institution Division, Department Division of Vehicular Systems Department of Electrical Engineering Linköpings universitet SE-581 83 Linköping, Sweden	**Datum** Date 2012-06-11

Titel   En metod for skattning av sotmassa i en DPF med RF-baserad sensor
Title   A Method for Estimating Soot Load in a DPF Using an RF-based Sensor

Författare John Hansson och Victor Ingeström
Author

Sammanfattning
Abstract

The European emission standard is an EU directive which describes what emission limits car manufactures are required to meet. In order to meet these requirements car manufacturers use different techniques and components. In a modern diesel automobile a Diesel Particulate Filter (DPF) is used to gather soot from the exhausts. As soot accumulates in the DPF, the back pressure increases and the capability to hold more soot decreases. Therefore the DPF continuously needs to get rid of the stored soot. The soot is removed through a process called regeneration. In order to optimize when to perform regeneration, it is vital to know the amount of soot in the filter.

A method for estimating the soot mass in a DPF using a radio frequency-based sensor has been developed. The sensor that has been studied is the Accusolve soot sensor from General Electric. A parameter study has been performed to evaluate the parameters that affects the sensor's output. Parameters that have been studied include positioning of the sensor, temperature in the DPF, flow rate through the DPF and distribution of soot in the DPF. Different models for estimation of soot mass in the DPF has been developed and analyzed.

An uncertainty caused by removing the coaxial cable connectors when weighing the DPF has been identified and methods for minimizing this uncertainty has been presented. Results show that the sensor output is sensitive to temperature, soot distribution and position, and also show some sensitivity to the flow rate. An ARX model, with only one state, is proposed to estimate the soot mass in the DPF, since it gives the best prediction of soot mass and showed good resistance to bias errors and noise in all the input signals.

Abstract

The European emission standard is an EU directive which describes what emission limits car manufactures are required to meet. In order to meet these requirements car manufacturers use different techniques and components. In a modern diesel automobile a Diesel Particulate Filter (DPF) is used to gather soot from the exhausts. As soot accumulates in the DPF, the back pressure increases and the capability to hold more soot decreases. Therefore the DPF continuously needs to get rid of the stored soot. The soot is removed through a process called regeneration. In order to optimize when to perform regeneration, it is vital to know the amount of soot in the filter.

A method for estimating the soot mass in a DPF using a radio frequency-based sensor has been developed. The sensor that has been studied is the Accusolve soot sensor from General Electric. A parameter study has been performed to evaluate the parameters that affects the sensor's output. Parameters that have been studied include positioning of the sensor, temperature in the DPF, flow rate through the DPF and distribution of soot in the DPF. Different models for estimation of soot mass in the DPF has been developed and analyzed.

An uncertainty caused by removing the coaxial cable connectors when weighing the DPF has been identified and methods for minimizing this uncertainty has been presented. Results show that the sensor output is sensitive to temperature, soot distribution and position, and also show some sensitivity to the flow rate. An ARX model, with only one state, is proposed to estimate the soot mass in the DPF, since it gives the best prediction of soot mass and showed good resistance to bias errors and noise in all the input signals.

Acknowledgments

We would like to thank a number of people for help and support during this master's thesis.

A special thanks to our supervisors at LiTH, Daniel Eriksson and Oskar Leufvén, for their help, guidance and feedback.

Our supervisor Anna Hägg at Volvo Cars is gratefully acknowledged for her support during this thesis.

Our colleagues at Volvo, with a special thanks to Ken Madsen, Jonas Karrin, Christian Vartia, Anders Botéus and Niklas Sergrén who all helped us when we were new at Volvo.

Finally we would like to thank Lars Eriksson and the vehicular systems department of LiTH for making this thesis possible.

Contents

Glossary

S_{11} The reversed input reflection coefficient, denotes the relation between input and output voltage for the first antenna.

S_{21} The forward gain from the transmitter antenna to the receiver antenna.

Downstream   When a location is referred to as being downstream from a component, it means that it is on the side of the component which is furthest away from the engine when following the exhaust flow.

Isokinetic sampling   A method for collecting airborne particulate matter in a flow. By leading some of the main flow into a separate collector-channel while making sure both the main- and the collector-channel has the same flow velocity.

Regeneration   Regeneration is the process where soot is oxidized into CO_2. There are two different kinds of regeneration; *Active regeneration* with oxygen - which is performed by heating the soot to more than 550°C and *Passive regeneration* with NO_2 - which occurs at lower temperatures (above 200°C).

Upstream   The opposite of downstream.

Acronyms

DOC   Diesel Oxidation Catalyst

DPF   Diesel Particulate Filter

MW   Microwave

OBD   On Board Diagnostics

PM   Particulate Matter

RF   Radio Frequency

Chapter 1

Introduction

The European emission standard is an EU directive which describes what emission limits car manufactures are required to meet. The current legislation called Euro 5 (valid from 2009), limits the emission of Particulate Matter (PM) to 5 mg/km, which is a decrease by 80% compared to the previous Euro 4, see [1]. PM consists mainly of soot particles from incomplete combustion but contains also inorganic ash forming compounds such as *Ca, Zn, P* and sulfates [3, 12].

The main technology used for achieving reduced PM emissions is the Diesel Particulate Filter (DPF), which is also the technology assumed for PM filtering when the emission limits where set for Euro 5, see [2]. There is a lot of different types of diesel particle filters on the market, the most commonly used is the ceramic wall flow filter.

This thesis focuses on a ceramic wall flow filter used in a Volvo diesel car in 2011. Figure 1.1 shows a simple schematic of some of the main components between the engine and the DPF. When the exhausts pass the DPF, most of the PM is getting trapped inside the DPF (up to 99%). As the soot accumulates inside the DPF, the back-pressure rises and the capability to hold more soot decreases. Therefore the DPF continuously needs to get rid of the stored soot. Soot is removed through oxidation, which is also referred to as *regeneration*. Regeneration turns soot into CO_2.

There are two types of regeneration; *passive* and *active regeneration*. Passive regeneration starts at a lower temperature ($\approx 200°$C) than active regeneration ($\approx 550°$C). The passive regeneration requires NO_2 and the rate of passive regeneration can be increased by increasing the amount of NO_2 in the DPF. To increase the amount of NO_2, a Diesel Oxidation Catalyst (DOC) is placed *upstream* from the DPF, see Figure 1.1. The main purpose of the DOC is however to oxidize HC and CO. In the DOC, NO is oxidized into NO_2 as the exhausts passes. Active regeneration, which is soot oxidation by O_2, requires that the temperature increases to above 550°C. This is done by late injection of fuel in the cylinders. The soot load increases faster than passive regeneration can handle. Thus, active regener-

ation is needed about every 1000 km. Active regeneration is desired only at an appropriate soot load. If the soot load is too low when using active regeneration, the result will be unnecessary fuel consumption and increased emissions of CO_2. On the other hand, if performed at a too high soot load, the temperature required to burn out the soot may crack or even melt the filter, see [12].

Figure 1.1. A schematic view of how the exhausts travel from the engine to the Diesel Particulate Filter (DPF). In this figure the Diesel Oxidation Catalyst (DOC) is closely coupled with the DPF, in other configurations they may be separated. A pressure sensor measures the pressure drop Δp over the DPF. The pressure drop is then used together with the internal models to estimate the soot load during operation.

1.1 Problem formulation

Since regeneration is a critical phase, knowing when to regenerate is a key factor for minimizing fuel consumption and maximizing life-time of the components. Today, control algorithms, regulating when to regenerate, are based on knowing the accumulated soot mass trapped inside the DPF at a given time. Currently, Volvo uses on-line models in combination with a pressure sensor that measure the pressure difference between *upstream* and *downstream* of the DPF to estimate the soot load. These estimation models need calibration when used in a new setup. To be able to calibrate the models, the soot load of the DPF must be known while tuning the parameters. The pressure drop measured in the differential pressure sensor is a function of exhaust flow rate, soot characteristics and packaging, see [27]. It is difficult to know the soot distribution in the filter and therefore the mass estimation based on the differential pressure sensor can be less accurate for certain types of driving cycles. Today, the DPF is removed and weighed to measure the soot load. This is a very time consuming job and therefore Volvo is looking

at a solution using the "Accusolve advanced diesel particulate filter soot sensor" from GE, henceforth referred to only as the soot sensor, see [5]. The soot sensor should be able to indirect measure the soot load by measuring the attenuation of radio waves at resonance frequencies. After recording of data, the soot load should be estimated. If the soot sensor gives a reliable measurement of the soot load, it will save a lot of time in the process of calibration of the models. Improved accuracy in the models could also lead to improved emissions and/or reduced fuel consumption.

1.2   Goals

The goal in this thesis is to evaluate the soot sensor and to develop a model for soot estimation. The purpose of the sensor is to measure the mass of the trapped soot in the DPF rather than estimating it when the vehicle is used in field tests. This information can then be used to calibrate the internal models, preparing the car for production. The goals can be summarized in the following bullets:

- A soot estimation method based on the soot sensor [5] shall be developed.

- The performance of the developed method compared to weighed soot load shall be evaluated.

- A parameter study is to be performed, taking into account some of the parameters that may affect the measurement of the sensor. The parameters involved are: temperature, flow rate, soot characteristics and positioning of the sensors.

- A sensitivity analysis shall be performed with respect to the parameters above, to evaluate the measurement method.

- Given the developed method and performed analyses, a recommendation on how to use the developed method to minimize uncertainties is to be suggested.

1.3   Approach

The approach can be divided into three parts; First, planning and performing of a series of tests to gather data, followed by analysis of the data. Finally a method for the usage of the sensor will be developed.

1.3.1   General approach

Based on previous research in the field of mass detection using RF/MW-sensors, two main approaches was tested. The theory behind the first approach is to simply see how the attenuation of RF waves are influenced by the amount of soot load,

then mathematically describe the correlation. To measure the degree of attenuation, the forward gain S_{21} was measured for some different frequencies.

The second approach is based on the research of resonance frequencies. In this approach, the DPF is seen as a perfectly conducting metal cavity resonator. As soot accumulates in the filter, the dielectric properties of the filter is affected, see [13]. The resonance frequency f_r of a cavity resonator is shifted depending on the dielectric and conducting properties of the housing and its contents. Research has shown that these shifts can be used as a correlation for computing the load, see [13, 23]. The second approach uses the forward gain S_{21} and uses the changes in the gain at certain frequencies, which is a sign of resonance.

1.3.2 Planning and performing the tests

For each test, a test plan was made and followed during the test. The first test was a simple setup of the sensors without any other engine components involved to make sure all signals that where needed could be read correctly. This was just to investigate how the sensor works and to setup the measurement system.

The second test was performed in a test rig and engine parameters where changed during the test. Different driving scenarios was tested to evaluate if different soot load distributions would result in the same measurement values. The test plan for the second test included the engine operating points for the test and a list of data that should be collected during the test.

When the second test had been evaluated, the third test was planned based on the outcome of the second test. The test plan for the third test contained the same parts as the second test. The third test was performed to collect data used for estimation of the models. For all tests, except the first one, the DPF was weighed before and during the test. During the tests the DPF was removed and weighed for validation. Data collection of engine parameters was made with the software applications INCA. Data was evaluated and analyzed using MATLAB.

1.4 Methods for measuring soot load

Measuring the soot inside the DPF is not easy, and thus there has been different methods developed for soot estimation.

Measuring the soot concentration in the exhaust flow is a well-tested approach, see [10, 19, 15]. This kind of measurement can be accomplished by placing a sensor downstream the DPF with two electrodes; one is energized while the other is not. Initially the resistance between the electrodes is assumed to be very high, but as soot start to build up between them the resistance decreases. This approach is often used to gather knowledge about the state of the DPF when applied in On Board Diagnosis (OBD) or to monitor emissions directly in the exhaust. There are uncertainties whether the measurements are accurate enough for other applications

than OBD, considering that it does not measure the soot load in the actual filter.

Another approach is to extract a sample of the raw exhaust from the engine and run it through a smaller sample filter, see [9]. This method is intended for *isokinetic sampling* during steady state operation and can be a good way to gather knowledge about the soot accumulation at those conditions.

In order to get more information about the soot distribution in the filter a method with an infrared camera has been tested in [20]. The camera records the soot distribution during regeneration on the filter mainly for the purpose of optimizing the geometry of the filter for a more even distribution of soot inside the filter. In theory, this method could also be used to measure the soot mass in the DPF, but since regeneration is needed for the camera measurements, an extensive number of regenerations will be needed to gather enough data to be able to calibrate the models.

An interesting approach, that could be an alternative to the one studied here, is to measure the resistance directly over a few channels in the filter. An increase in soot load will result in a resistance decrease, see [14]. With this method, a number of electrode pairs are placed along the sides of the filter from inlet to outlet. This method can not only measure the soot load but also the distribution of the soot inside the filter. The down side of this method, is that assumptions has to be made regarding the amount and distribution of soot between two electrode pairs.

The approach studied here is to measure the soot load with a radio frequency based sensor. As the DPF is loaded with soot the permittivity and conductivity of the filter change. This should be observable via resonance frequency shifts or via changes in the attenuation of the radio waves, see [13]. This approach has also been used to control the active regeneration of a DPF in city buses, see [28]. The correlation between the soot load and the radio frequency signal has been shown to be close to affine when measurements where performed at approximately the same temperature, see [24].

1.5   Other applications where electromagnetic wave sensors are used

Radio frequency-based sensors have a wide range of use for detecting presence of a specific substance. When used inside a large enough cylindrical metal container, the container acts as a cavity resonator, guiding the electromagnetic waves and thus for certain frequencies creating standing waves that easily can be measured. At different frequencies, RF absorbability differs for different substances. By choosing a frequency which responds only to an interesting substance, electromagnetic waves may pass through other materials unaffected, making them literally "invisible" to the RF sensor. By observing the electrical permittivity, a direct measurement of the corresponding substance can be made.

The amount of oxygen loading in a three-way catalyst have been successfully measured by using the absolute value of the reflection coefficient S_{11} for detection of resonance frequencies and then observing how the resonance frequencies shift with increased loading [21, 22].

Using the same basic concept, *NH$_3$* (Ammonia) loading in an SCR catalyst have been analyzed using microwaves. The result was that by choosing an appropriate frequency the cross-sensitivity towards water was almost reduced completely. Reproductivity and measurements where satisfying using only one probe, see [23].

Research has shown that this method can be used not only in the automotive sector, but also in other fields such as in the biological sector, where microwave sensors have been used to measure total mass and moist content inside a single soybean, see [16].

Chapter 2

Theory

In this chapter some of the theory used in this report is presented. The theory described here involves general information about the Accusolve soot sensor, a brief introduction to the scattering matrix as well as the theory for the estimation methods which will be used later in this report.

2.1   Accusolve soot sensor

The Accusolve soot sensor from General Electric is based on radio wave technology. The dielectric properties of soot differ from that of the filter material and the ash in the filter. By measuring the attenuation of the RF signal within the DPF canister the soot load should be detectable. In Figure 2.1, a schematic overview of the sensor setup is shown. Note that the temperature (3) in the figure is not included in a production car, but is used to compare the difference in temperature upstream and downstream of the DPF. The transmitting antenna is positioned upstream from the DPF and the receiving antenna is positioned downstream from the DPF. Both antennas are connected to the soot sensors micro controller that calculates the forward gain S_{21}. The operating frequency of the sensor ranges from 2.1 Ghz to 2.2 Ghz. The forward gain is calculated at discrete frequencies with steps of 0.5 Mhz. In Figure 2.2 an example of the sensor output is shown.

The sensor provides both serial data and CAN bus data. For this project only the serial data will be used, the CAN bus data is used for GE's soot mass algorithm that is not in use. The serial data from the sensor include an array of forward gains for each discrete frequency step as well as standard deviation, max and min values of the noise and the average gain for all the discrete frequencies.
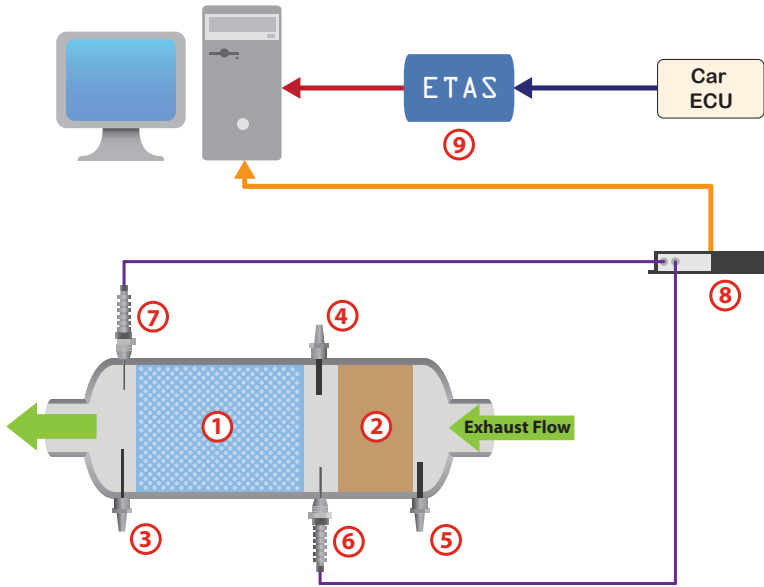
Figure 2.1. Schematic system setup. (1) DPF, (2) DOC, (3) Temperature sensor, (4) Temperature sensor, (5) Lambda sensor, (6) RF transmitter, (7) RF reciever, (8) Soot sensor micro controller, (9) ETAS 690 communication unit for the car ECU.
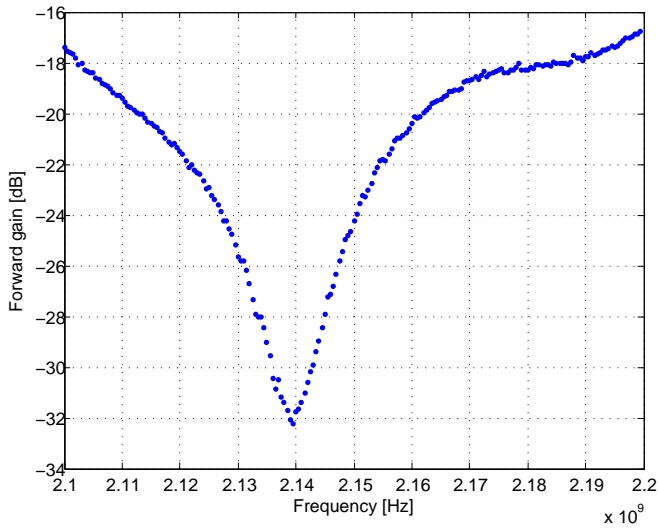

Figure 2.2. A single output from the soot sensor. The output is the forward gain for 200 discrete frequencies ranging from 2.1 GHz to 2.2 GHz.

2.2   The Scattering matrix

For more than 60 years, the scattering matrix and its parameters have been used for characterization, modeling and analysis by the microwave community, see [11]. It is a very wide subject and in this section, a brief summary of the key features needed to define the scattering matrix is presented. When using an arbitrary number of antennas in a system, the system is referred to as a multi-port or N-port, where N is the number of antennas used. A port with a transreceiver antenna can both induce and receive waves. In this thesis, the focus is on a 2-port system with two transreceiver antennas.

If the transverse wave direction through a waveguide is defined as the z-axis, the transverse components of the total fields $\mathbf{E}$ and $\mathbf{H}$ in a uniform waveguide, propagating a single mode, can be derived from Maxwell's equations and expressed according to [8] as

$$\mathbf{E_t} = c_+ e^{-\gamma z} \mathbf{e_t} + c_- e^{+\gamma z} \mathbf{e_t} \equiv \frac{v(z)}{v_0} \mathbf{e_t} \tag{2.1}$$

and

$$\mathbf{H_t} = c_+ e^{-\gamma z} \mathbf{h_t} - c_- e^{+\gamma z} \mathbf{h_t} \equiv \frac{i(z)}{i_0} \mathbf{h_t} \tag{2.2}$$

where v and i are called the *waveguide voltage* and *waveguide current*. The normalizing parameters v_0 and i_0 have the units voltage and current respectively, and are introduced to maintain appropriate units for the fields $\mathbf{H_t}$, $\mathbf{E_t}$, $\mathbf{h_t}$ and $\mathbf{e_t}$. γ is the modal propagation constant and is defined as a complex number $\gamma \equiv \alpha + j\beta$.

The forward and backward waveguide voltage can be expressed as $v^+(z) = c_+ v_0 e^{-\gamma z}$ and $v^-(z) = c_+ v_0 e^{-\gamma z}$ respectively. Similarly $i^+(z) = c_+ i_0 e^{-\gamma z}$ and $i^-(z) = c_+ i_0 e^{-\gamma z}$ are introduced and referred to as forward and backward waveguide current, see [8].

How radio frequency energy propagates between multiple ports can be described as

$$\bar{b} = \mathbf{S} \cdot \bar{a} \tag{2.3}$$

Where $\mathbf{S}$ denotes the *scattering matrix* and the vectors $\bar{a}$ and $\bar{b}$ are the forward and backward voltage respectively, i.e. $a \equiv v^+$ and $b \equiv v^-$, see [8].

For example, if two antennas are used, (2.3) is given by

$$\begin{pmatrix} b_1 \\ b_2 \end{pmatrix} = \begin{pmatrix} S_{11} & S_{12} \\ S_{21} & S_{22} \end{pmatrix} \begin{pmatrix} a_1 \\ a_2 \end{pmatrix} \tag{2.4}$$

A *scattering parameter* S_{ij} in the scattering matrix describes the relation between the waveguide voltage from port i to port j, both in aspect of amplitude and phase. Each scattering parameter S_{ij} can be determined by

$$S_{ij} = \frac{b_i}{a_j} \bigg|_{a_k = 0, k \neq j} \tag{2.5}$$

when all ports except a_j are terminated with matched loads, meaning only port j induces waves, see [11]. When talking about the gain, only the amplitude of S_{ij} is considered, not its phase.

The output from GE's RF soot sensor is the forward gain S_{21} converted to dB, for a set of pre-defined discrete frequencies.

2.3 Model estimation using linear least squares

A least squares formulation of an estimation problem is used to make a regressive fit based on minimizing the squared residual $r(n) = y(n) - f(u(n), A)$ where $y(n)$ is the measured output signal, $f(u(n), A)$ is the function which is to be fitted to the data and each element of the row-vector U are the measured input signals and A are the unknown parameters. The optimal solution to the least squares problem is the value of A that minimizes S in

$$S = ||Y - UA||^2 = \sum_{n=1}^{k} \Big(y(n) - f(u(n), A) \Big)^2 \tag{2.6}$$

where

$$Y = \begin{pmatrix} y(n) \\ \vdots \\ y(n+k-1) \end{pmatrix} \quad U = \begin{pmatrix} u_1(n) & \dots & u_i(n) \\ \vdots & \ddots & \vdots \\ u_1(n+k-1) & \dots & u_i(n+k-1) \end{pmatrix} \quad A = \begin{pmatrix} a_1 \\ \vdots \\ a_i \end{pmatrix}$$

and k is the number of measurements and i is the number of input signals, see [7].

By using an linear function $f(U, A)$, thus describing the output y(n) as

$$\hat{y}(n) = f(U, A) = a_1 u_1(n) + a_2 u_2(n) + \dots + a_n u_n(n) \tag{2.7}$$

the solution A which minimizes (2.6) can be computed explicitly as

$$A^* = (U^T U)^{-1} U^T Y \tag{2.8}$$

The solution to (2.8) can then be used in (2.7) for the estimation. UA^* is the best linear predictor of Y according to the least squares method, see [7].

2.3.1 L1-Norm regularization

To reduce complexity of the predictor estimated above, a method called the L1-Norm Regularization (lasso function) can be used to determine which signals that have the most influence on the output signal, see [26]. The lasso function can be described as an extension of the least squares problem, with a penalty λ for using a parameter $a_i \neq 0$, see (2.9). By increasing λ, dominant correlations can be identified. The lasso function can be described as

$$\min_A ||Y - UA||^2 + \lambda |A|. \tag{2.9}$$

2.4   Linear black box models

A model is an attempt to reproduce a prediction of the output signal y as a function of the input signals u. A black box model has no physical interpretation but rather replicates the behavior seen in measured data. A black box model can be produced in multiple ways; by fitting data to a linear or nonlinear model, like ARX, NARX, ARMAX, OE, BJ or using spectral analysis, see [17]. When creating a black box model, some of the gathered data is used for estimation, while the unused data is used for validation of the model. In this section some of the most common linear black box models are described. The choice of only focusing on linear models to estimate soot mass is based on previous research where the relation between forward gain and soot have shown linear behavior, see [28].

In Figure 2.3, a graphical representation of the black-box model structures can be seen. In the following section a short description of each model is presented. More about the model structures can be read in [18].
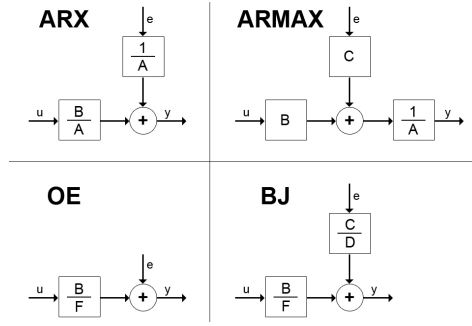

Figure 2.3. Model structures used for developing linear black-box models

An ARX (Auto Regressive eXternal input) model is a simple model where the white noise e, is modeled a transfer function with the same denominator as the the system dynamics.

An ARMAX (Auto Regressive Moving Average eXternal input) model gives more freedom to the model than an ARX model by using an extra transfer function numerator to describe the dynamics of the white noise e in the system.

An OE (Output Error) model assumes that that the model can be described as if the white noise e is added directly to the output value.

A BJ (Box Jenkins) model is most general and offers the most freedom of the four models described but is also the hardest to estimate. The model uses a separate transfer function with both a numerator and a denominator to describe the influence from the white noise e.

Chapter 3

Experiments

Two series of experiments were constructed and performed. The first series was performed in a car and the second in a test cell. The experiments in the car were performed to evaluate the sensors ability to detect soot. The experiments performed in the test cell were made to evaluate the sensor's dependence of temperature, soot load, flow rate, sensor position and soot distribution.

3.1   Sensor measurement system

The antennas were mounted in the mounting holes welded on the DPF and connected to the sensor box. The sensor box's serial output cable were connected to a laptop via an RS-232 to USB converter. Recording and decoding of data was done by a script in Microsoft Excel.

3.2   Measuring soot mass

All weight measurements were made with a hot DPF (temperature over 100°C in the filter). This was made to prevent water from condensing in the filter and therefore increasing the weight of the DPF.

3.3   Initial experiments in car

A real field test for highway driving was performed to investigate the detectability of soot. A 2.0 liter, automatic transmission, front wheel drive Volvo XC70 was used. No weighing of the DPF was performed during this test. Instead the simulated soot mass was used as a reference for detecting increased soot load.

High soot build up in the DPF can be achieved by running the engine at low engine speeds with high loads, see [25]. During the highway cycle the torque was demanded in a transient way by requesting maximum torque with the acceleration pedal for about one to two seconds, then letting go for approximately 3 seconds,

making sure the car maintained the same speed and were held at a low engine speed. These were factors that kept the soot build up at a high rate. In Figure 3.1 the soot sensor output can be seen for the highway drive cycle for approximately 40 minutes, where dark curves are early measurements and bright are late measurements. Figure 3.1 shows that different frequencies behave differently during soot build up. Although, the average gain of all frequencies decreases during soot build up.

In the figure, it can also be seen that the approach of using the resonance peak shift can not be used. At low soot load, a peak can be seen at 2.13Gzh in the output signal, which could be a result of resonance. However as the soot load increases the peak disappears.

Figure 3.1. Soot sensor output when driving in an urban area with an automatic transmission Volvo XC70 2.0 liter diesel car for approximately 40 minutes. The car was driven at highest gear. The lowest engine speed allowed, without letting the transmission shifting down, was used to produce as much soot as possible. Dark curves are early measurements and bright are late measurements. The figure shows that different frequencies behave differently during soot build up. Although, the average gain of all frequencies decreases during soot build up.

3.4 Engine and test cell specifications

The engine used in the test cell is a 2.0 liter diesel engine with automatic transmission. Specifications of the motor can be seen in Table 3.1. The test cell was equipped with a dynamometer to control the load on the engine.

INCA was used to monitor the engine parameters and to control the ECU. The

Engine Specifications		
Cylinders	5	[-]
Bore	81	[mm]
Stroke	77	[mm]
Power Output	120	[kW]
Max. Torque	400	[Nm]

Table 3.1. Specifications for the engine used in the test cell

ECU controls when to trigger regeneration and which operation mode the engine is currently in. By modifying these triggers, or by manually setting operation modes, unwanted regenerations could be prevented or forced at any time.

3.5 Test cell experiments

Two different configurations for the antenna positions were used in the experiment to evaluate positioning of the antennas, see Figure 3.2. The sensor response were studied for several different engine operating points. To build up soot at a relatively high speed, a cycle with five different engine operating points was used. Each operating point runs for one minute and then switches to the next and the cycle runs repeatedly. Engine operating points for the soot build up cycle are shown in Table 3.2.

Operating points for soot build up cycle			
	Engine speed [rpm]	Velocity [km/h]	Throttle [%]
1	2100	120.5	18.0
2	1500	86.0	13.0
3	1900	107.0	13.5
4	1300	72.0	16.5
5	2000	113.5	16.0

Table 3.2. Engine operating points for soot build up cycle. Each operating point runs for one minute and then changes to the next.
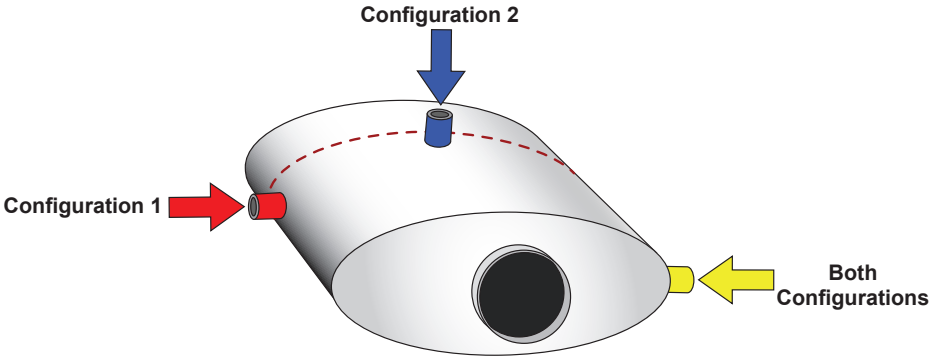
Figure 3.2. The two different configurations used in the sensor positioning experiment. The dashed line indicates where the gap between the DPF and the DOC is located.

To test the flow rate dependency of the RF-measurements, another cycle with five operating points was used, each point ran for five minutes. Each point had the same temperature at the inlet of the DPF in steady state but with different flow rates, see Table 3.3. For the temperature dependency test, a similar cycle with six different operating points were used, each point ran for ten minutes. All points had the same flow rate but with varying temperatures, see Table 3.4.

Operating points flow dependency experiment					
	Eng. spd [rpm]	Velocity [km/h]	Throttle [%]	Temp. [°C]	Flow [m^3/h]
1	1750	100.0	12.2	305	125
2	2150	120.0	14.2	305	160
3	2300	130.0	16.0	305	180
4	1400	80.0	11.5	305	100
5	2450	140.0	17.3	305	225

Table 3.3. Engine operating points for flow rate dependency experiment. The temperature is measured in the exhaust flow at the inlet of the DPF and the flow rate is the calculated flow rate through the DPF.

The soot distribution dependency experiment was performed in two ways. In the first test, a full DPF is regenerated to about half the soot load. Then the soot build up cycle is continued until the DPF is full again. The DPF is weighed periodically and data from the sensor is recorded throughout the experiment. The second test was performed using a recording of an actual taxi trip in Stockholm, which includes many starts and stop of the engine. The experiment started with

an empty DPF and ran until the DPF was almost full. These two experiments were expected to result in different soot distributions due to differences in flow rate through the DPF and temperature in the DPF and are thus compared, to evaluate the effect of soot distribution.

	Eng. spd [rpm]	Velocity [km/h]	Throttle [%]	Temp. [°C]	Flow [m³/h]
Operating points temperature dependency experiment					
1	2200	125.0	10.0	210	120
2	1200	66.0	13.5	360	120
3	1400	80.0	12.5	340	120
4	1600	90.0	12.0	320	120
5	1800	100.0	11.5	295	120
6	2100	120.0	11.0	245	120

Table 3.4. Engine operating points for temperature dependency experiment. The temperature is measured in the exhaust flow at the inlet of the DPF and the flow rate is the calculated flow rate through the DPF.

Regenerations were performed at 2800 rpm and 16% throttle. This point is suitable for regeneration since it has a high flow rate which helps the hot exhausts to spread faster throughout the filter. At this point, lambda has a relatively high value and therefore the exhausts contain a lot of oxygen which speeds up the regeneration process.

Chapter 4

Experiment analysis and soot mass estimation

In this chapter the results from the performed experiments are presented and analyzed. The chapter contains the results from experiments, where the parameters; sensor position, soot load, temperature, flow rate and soot distribution are analyzed. A soot-estimation model described by (2.7) was developed, this model is henceforth referred to as the *average gain-model*, where A was estimated using least squares. Four soot-estimation models where also developed based on the black-box models in section 2.4.

4.1 Results from experiments

In this section the results from the experiments in the test cell will be presented as well as an analysis of the results. The sensor output is compared directly to the weighed soot load as well as other parameters that could affect the output from the sensor. The other parameters include temperature at inlet of the DPF, flow rate through the DPF and position of the antennas.

4.1.1 Position

The purpose of this experiment is to evaluate which position for the antennas that is the most suitable. The positioning of the antennas affects the base forward gain when the DPF contains no soot. A low damping for an empty filter is desirable as the soot sensor will be better at detecting changes in soot load at stronger signals according to [4]. In Figure 4.1 the average gain from the sensor output with configuration one and two is shown. Figure 3.2 shows the positions of the antennas for the two different configurations.

As shown in Figure 4.1, the forward gain is generally higher for the first configuration than for the second one. This is desired for the best possible output from the

sensor system, see [5]. Therefore the configuration used will henceforth be the first configuration where the antennas are positioned on opposite sides of the DPF, see Figure 3.2.
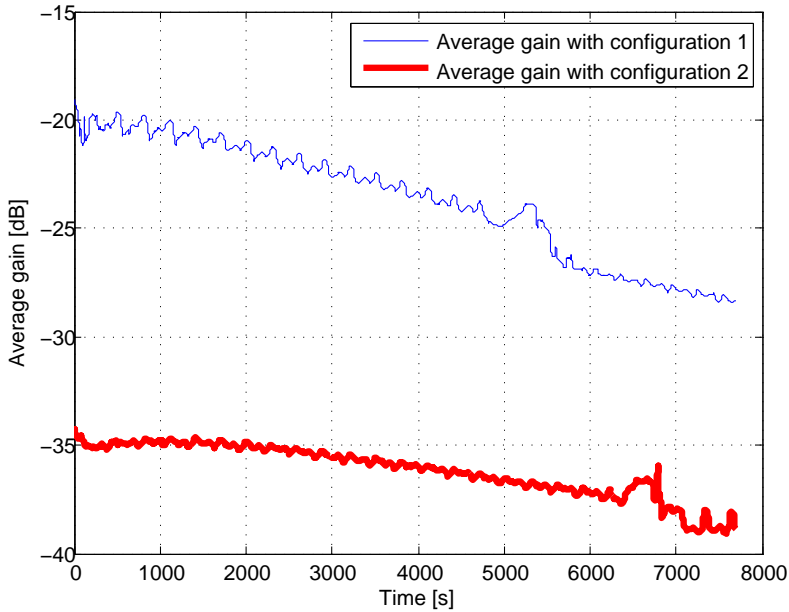

Figure 4.1. Average gain from the sensor as a function of time with antennas mounted in configuration one and two.

4.1.2 Soot load

Here, the results from the soot load dependency test are shown. In Figure 4.2, the sensor output as a function of time and the weighed soot load as a function of time are shown. Figure 4.2 shows an example of the soot build up.

As can be seen in Figure 4.2 the average gain decreases when the soot load increases. The soot load in Figure 4.2 is plotted negatively for easier comparison with the average gain. A soot load between 0 and 20 gram corresponds to a change in average gain from -20 dB to -32 dB. Note that the average gain of the soot sensor flattens out with increasing soot mass.
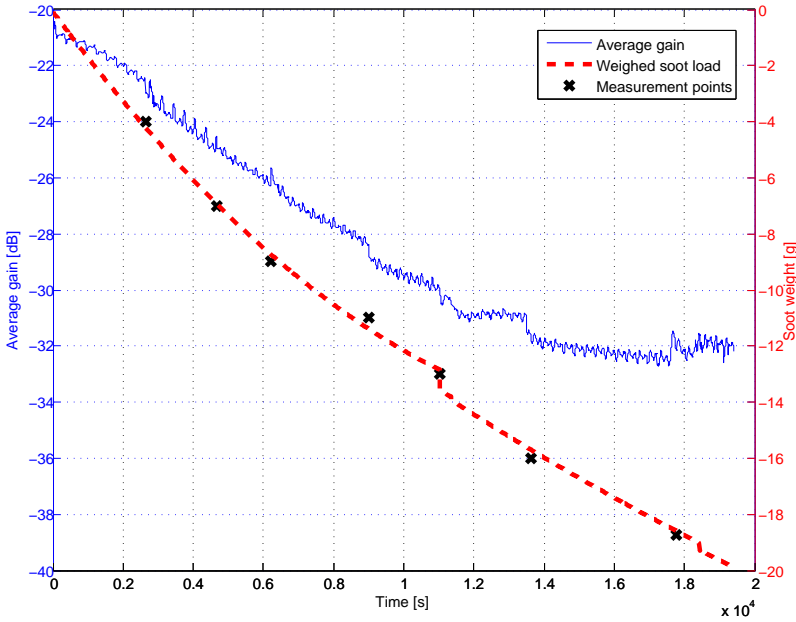
Figure 4.2. Average gain from the sensor as a function of time and weighed soot load as a function of time. The weighed soot load in the plot is curve-fitted to the measurement points using a quadratic function, this will be discussed later in section 4.2.1. After the weighing at 11000 seconds, the sensor malfunctioned and a part of the measurements have therefore been cropped to exclude the faulty data.

4.1.3   Temperature

The temperature of the antennas is a parameter that could affect the measurement signal according to [24] and this parameter will therefore be studied. There is no temperature sensor at the antenna, thus the temperature sensor upstream of the DPF is used as an approximation of the temperature, see element 4 in Figure 2.1. The temperature sensor is also placed in the exhaust flow but more centered than the RF-antennas.

In Figure 4.3, the temperature and the average gain as a function of time is shown. The average gain in Figure 4.3 is detrended using MATLAB's command *detrend*. The command *detrend* estimates and removes the linear trend in the data.

In Figure 4.3, it is shown that the measurements of the average gain are clearly correlated with the temperature measurements. The temperature in Figure 4.3 is plotted negatively for easier comparison with the average gain. An increase in temperature lowers the average gain of the soot sensor. When temperature changes from 220°C to 380°C the average gain changes about 4 dB. The results

here shows that when trying to estimate soot mass, the effect of the temperature must be taken into consideration.
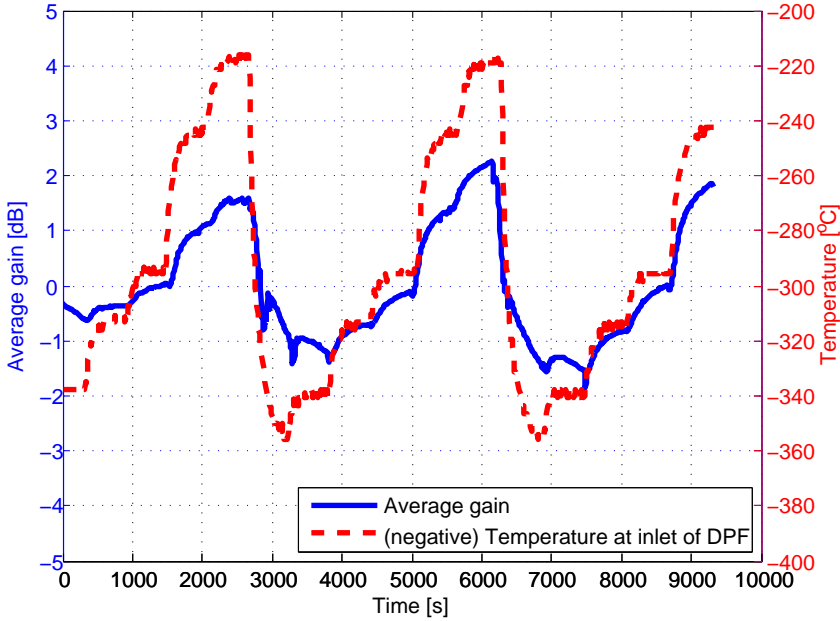

Figure 4.3. Average gain from the sensor as a function of time and temperature at inlet of DPF as a function of time.

4.1.4   Flow rate

The flow rate through the DPF is analyzed in this section. There is no sensor measuring the flow rate through the DPF but there is a calculated flow rate available. The computed flow rate value depends on the engine speed, the flow rate of air into the cylinders and the flow rate of fuel into the cylinders. In Figure 4.4, the flow rate through the DPF, as a function of time, and the average gain as a function of time are shown. The average gain in Figure 4.4 is detrended using MATLAB's command *detrend*.

In Figure 4.4, it is shown that the average gain is somehow dependent of the flow rate through the DPF, when the flow rate changes the average gain also change slightly. Comparing Figure 4.4 and Figure 4.3 shows that a change in temperature affects the sensor output more than a change in flow rate.
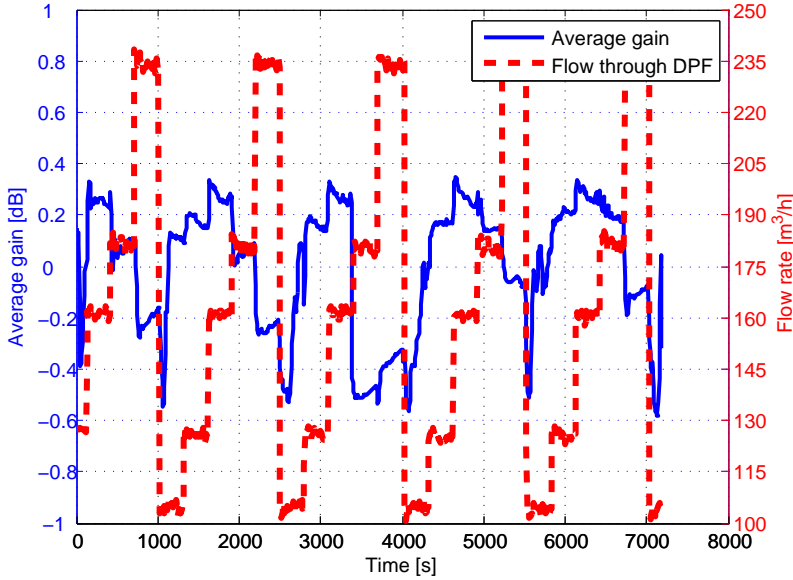
Figure 4.4. Average gain from the sensor and computed flow rate as a function of time.

4.1.5 Soot distribution

The soot distribution in the filter is a parameter that could affect the measurement signal, for example, if soot is distributed in the filter in such a way that the RF waves pass through a lot of soot, the forward gain will be dampened more than if the soot is distributed in such a way that the RF waves pass through less soot. In Figure 4.5, results from the soot distribution experiment are shown.

The average gain for measured soot of 14 to 18 grams is expected to be the same in the lower and upper plot if the sensor was not dependent of the soot distribution in the filter. The difference of distribution in the filter in the two plots in Figure 4.5 is hard to know in detail. One hypothesis is that in the lower plot, which is regenerated to about a half full DPF, more soot is burned out in the center of the filter and therefore the forward gain is higher since most of the radio waves travels through the center of the DPF. The rate of which the average gain changes in this interval is also higher in the lower plot in Figure 4.5. The difference could be explained with the DPF being more burned out in the center because of higher temperature there, thus more soot will pass through and get caught there.
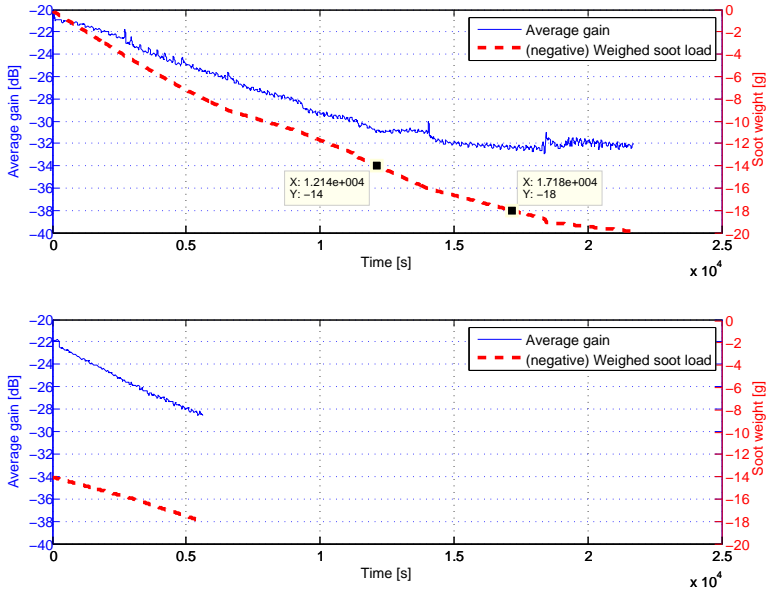
Figure 4.5. Data from the soot distribution dependency test. The upper plot shows the average gain when the DPF is regenerated to zero before gathering of data and the measured soot load. The lower plot shows the average gain when the DPF is regenerated to 14 gram before gathering of data and the measured soot load. Two markers are placed in the upper plot, these mark the same soot range as the lower plot. The results show that unknown soot distribution can not be detected by the soot sensor.

4.1.6 Frequency window analysis

The soot sensor output contains the forward gain for 200 discrete frequencies. In Figure 3.1, where the forward gain is plotted against the frequency spectrum it is shown that it is possible that looking at just a window of frequencies could give a better estimation of the soot load than looking at the average gain.

The purpose here is to analyze which frequencies in the soot sensor output that may contain the most relevant information. Some frequencies may be sensitive to soot while others may be more dependent on temperature. Therefore the frequency operating range were split into smaller intervals, i.e., "windows". The mean value of the forward gain for each window is then used as input signals to the L1-norm regularization method described in section 2.3.1. The window size can be chosen arbitrary, but choosing a too small window will result in more signal variance; choosing a too wide window on the other hand may dampen the effect of the frequencies which contain useful information. The window size were chosen to 10 frequencies, to balance uncertainty in the data and loss of information.

In the sections below, analysis for the average gain and the temperature are presented. This was made as a first step to evaluate if the L1-norm regularization method would select the same windows for different measurements series. The forward gain and the temperature have shown to have more influence than the flow for soot mass estimation, and was therefore evaluated as a first step. The second step would have been to also analyze the flow in a similar way. But since the outcome of the average gain and temperature analysis shows that neither window is better for soot estimation, no further analysis was performed.

The L1-Norm Regularization method, is used to penalize the windows that are not good enough for describing the output and calculate which windows is best for describing the selected output.

Gain window

In this section two series of measurements of soot build up where initial soot mass is 0 gram are analyzed using the L1-norm regularization method. To detect any non-linear behavior, the following inputs to the lasso function where also added as their respective squared values; the average gain for each window, the inlet temperature of the DPF, the flow through the DPF and the average gain for the entire frequency spectrum. The lambda parameter for the lasso function in (2.9) is varied to the point where the most dominant of the windows where selected.

In Figure 4.6 the result from the L1-Norm Regularization method when applied to the first series of measurements is shown and the result from the lasso function when applied to the second series of measurements is shown in Figure 4.7.

As seen in the parameter window for each series of measurements, the L1-Norm Regularization method does not choose the same windows for the two measurement series. This behavior is also repeated as lambda is varied in the L1-Norm Regularization method. This means that for estimating soot load there is not a set of windows that is better then any other for both sets of measurements. The conclusion of this is to use the average gain for the entire frequency spectra for determining soot load.
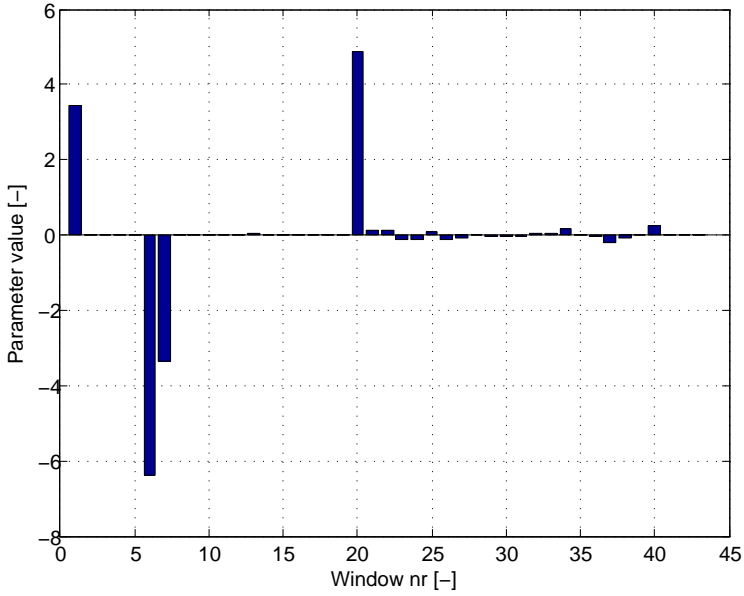
Figure 4.6. The result from the L1-norm regularization method applied to the first series of measurements. Each bar represent a window, windows 21-40 is the average gain squared and window number 41 and 42 is temperature and flow respectively.

Figure 4.7. The result from the L1-norm regularization method applied to the second series of measurements. Each bar represent a window, windows 21-40 is the average gain squared and window number 41 and 42 is temperature and flow respectively.
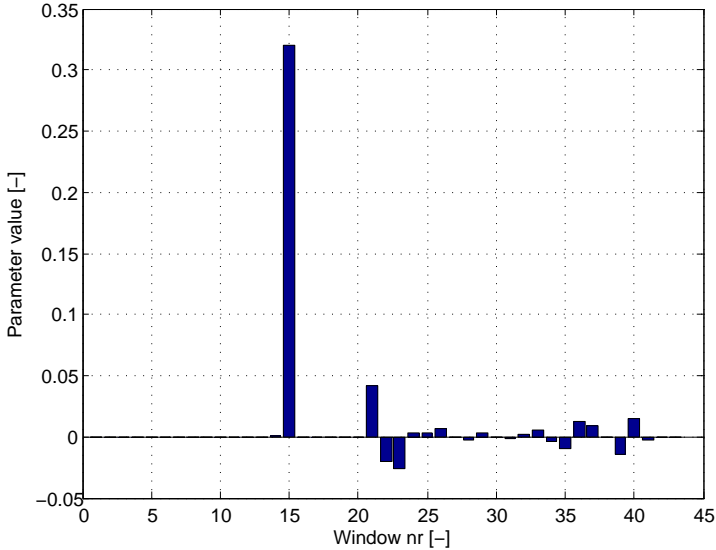
Temperature window

Here, a comparison between two series of measurements with respect to the relationship between temperature and average gain is made. Both series of measurement in this analysis have their frequency spectrum divided into 20 smaller windows as for the previous analysis. Inputs to the L1-norm regularization method are the average gain for each window and the output is the temperature at the inlet of the DPF. The lambda parameter for the lasso function is varied to the point where the most dominant of the windows were selected.

In Figure 4.8 and Figure 4.9, the result from the L1-norm regularization method when applied to the first and second series of measurements are shown. Comparing Figures 4.8 and Figure 4.9 shows that the L1-norm regularization method chooses different windows for different series of measurement. This result does repeat itself when lambda is varied and therefore it is concluded that there is not a set of windows for the average gain that is better then any other to describe the temperature dependency.
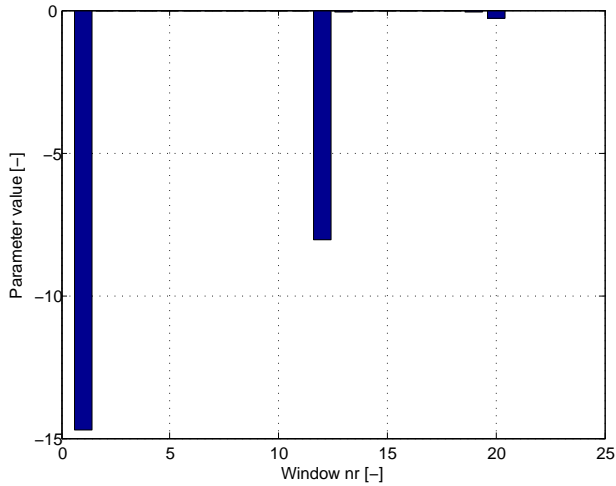

Figure 4.8. The result from the L1-norm regularization method applied to the first series of measurements, each bar represent a window. The temperature can be best described by windows 1 and 12 according to the L1-norm regularization method.
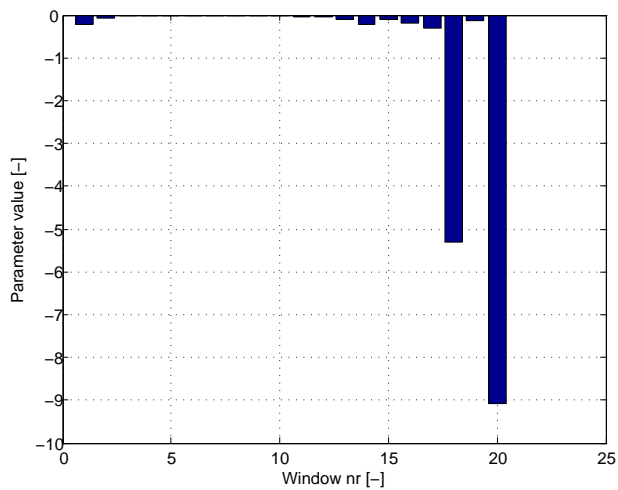
Figure 4.9. The result from the L1-norm regularization method applied to the second series of measurements, each bar represent a window. The temperature can be best described by windows 18 and 20 according to the L1-norm regularization method.

4.2   Modeling

In this section, the results from the performed experiments that are used to estimate a model for estimating the soot load as a function of average gain from the sensor, temperature upstream from the DPF and flow rate through the DPF are presented. The developed models estimated include the average gain-model and linear black-box models.

4.2.1   Pre-processing of measured data

As part of the pre-processing of the measured data, the weighed soot mass was curve-fitted using either an affine or quadratic function to better describe the soot build up process. The soot build up shows an affine behavior when the soot load is low. As the soot load increases, the rate of which the soot mass is accumulated in the DPF decreases and the behavior is better described by a quadratic function. Each of the measurement series which were collected at low soot loads, where approximated using a linear function, which best described their behavior. The measurement series which where either long enough for the soot load to start decaying, or showed decaying behavior (high soot loads) where instead curve-fitted using a quadratic function.

In addition to the curve-fitting of the weighed mass, the raw data from the measurements where pre-processed before being used for estimating the models. The pre-processing of data can be divided into three parts, see [17]:

- Removal of outliers (bad measurements) and unwanted peaks.

- Removal of high frequency disturbances above the frequencies of interest.

- Removal of drifts and offsets.

   The frequencies of interest for the soot build up are very low. Therefore no high-pass filtering in order to remove low frequencies was made on the collected data. This step can be skipped and instead letting the noise model take care of these possible low frequency disturbances, see [17].

Removal of outliers

In Figure 4.10, measured data is plotted as soot mass versus average gain to see which measurements that contain similar data and could be used for model estimation, and to detect outliers. The measurements are concentrated in a band running from -20 dB to -30 dB as soot builds up from 0 to 30 grams. The horizontal lines (marked in the figure) which goes down to -80 dB in forward gain are measurements when the engine has stopped and the coaxial cables were removed before stopping the measurement.

The measurements were trimmed so the faulty data (outliers), when the cables were removed, are excluded. Regenerations were also removed. The result can be seen in Figure 4.11, where the measurements also have been low-pass filtered using the method described in the next section.
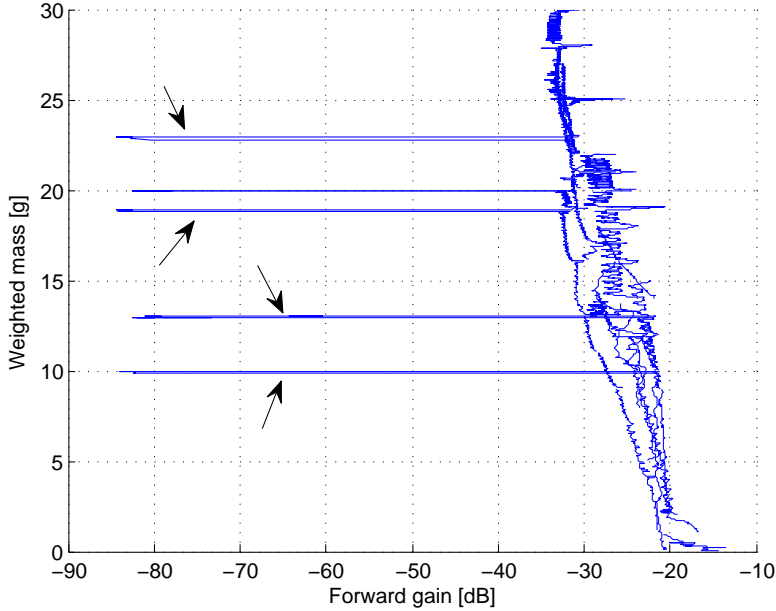

Figure 4.10. Soot mass in grams plotted against average forward gain in dB for the first position. The data is concentrated in a vertical slanted band. The horizontal lines, marked with arrows, are faulty data from when the engine is stopped and the coaxial cables were removed before the measurement was stopped.

Removal of high frequency disturbances

After removing outliers, the measured data was filtered using a 5th order butter-worth low-pass filter with a cut-off frequency of 0.005 rad/s. Filter orders between 1 and 7 were tested, where an order of 5 seemed to improve estimations the most. The filtering was made to remove frequencies above those of interest, see [18]. The chosen cut-off frequency gives a period time of 1257 seconds which is much shorter than needed for a single-run measurement. Shorter series of measurements tended to show an incorrect period time because of the shifts in gain caused by temperature when resuming an experiment. Therefore the cut-off frequency was chosen to ensure that changes in the start or final forward gain value before and after filtering was unaffected for all measured series. The filtered data can be seen in Figure 4.11.
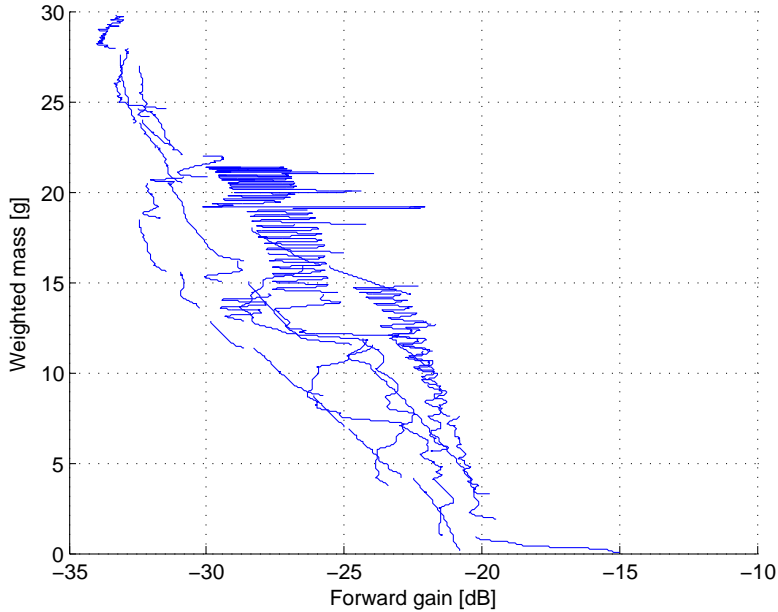
Figure 4.11. Mass in grams plotted against average forward gain in dB. The average forward gain is filtered using a 5th order butterworth low-pass filter with a cutoff frequency of 0.005 rad/s.

Estimation and validation split-up

The pre-processed data was split into two datasets. The first dataset was used for estimation and the second for validation. The estimation data consisted of a series of shorter measurements with varying soot ranges. The validation data was a soot build up from 3 to 30 grams measured over two days which gave the DPF time to cool off during the night.

4.2.2 Estimated soot gain model using least squares

The average gain-model was developed with the least squares algorithm, see section 2.3. When estimating the average gain-model using least squares, all estimation data available was used for estimating A in (2.8). Different time delays for the model were evaluated. The results show that even when including the latest 100 measurements, e.g. $Gain(t), \ldots, Gain(t-100)$, the estimated model was almost exclusively based on the single latest measurement. Only a minor increase in prediction performance was achieved by using past measurements to estimate soot mass. Therefore, only the latest measured signal was used as a parameter for estimation.

The parameters used for estimation of the soot weight in equation (2.6) are

$$Y = \begin{pmatrix} y(n) \\ \vdots \\ y(n+k-1) \end{pmatrix}$$

$$U = \begin{pmatrix} Gain(n) & Gain(n)^2 & Gain(n)^{-1} & Temp(n) & Flow(n) \\ \vdots & \vdots & \vdots & \vdots & \vdots \\ Gain(n+k-1) & \ldots & \ldots & \ldots & Flow(n+k-1) \end{pmatrix}$$

where $y(n)$ is the weighed soot load, $Gain(n)$ is the average forward gain S_{21} from the sensor, $Temp(n)$ is the temperature at the inlet of the DPF, $Flow(n)$ is the flow rate through the DPF and k is the number of measurements. The terms $Gain(n)^2$ and $Gain(n)^{-1}$ where included to capture possible non-linear relations between soot load and gain. The results however show that the estimation of the average gain-model use little or none of these available non-linear signals, see Figures 4.6-4.7. Similarly, non-linear flow and temperature where evaluated as inputs for estimation, with the same results. Therefore the average gain-model will not use the non-linear input signals for estimation.

In Figure 4.12 the result from the analysis with the least squares algorithm is shown. In the figure, it is shown that the model for estimation of the soot load can not really capture the characteristics of the curve for the weighed soot which is undesirable.
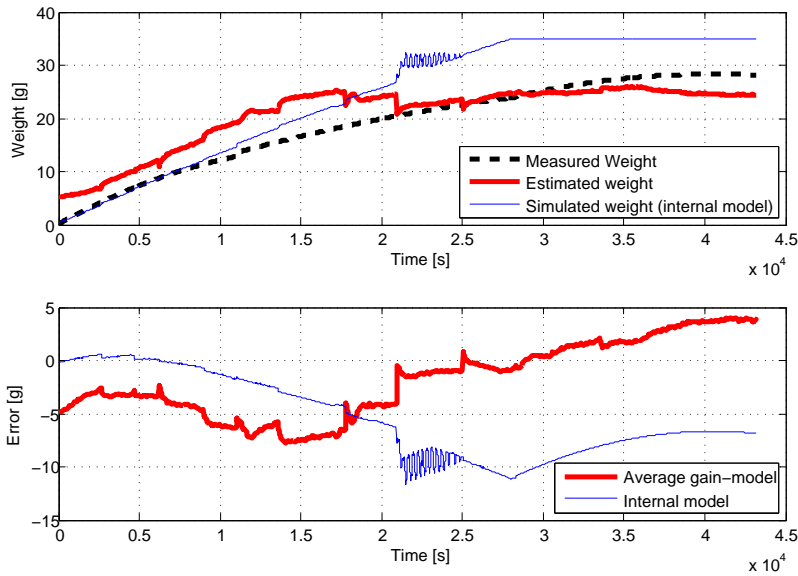
Figure 4.12. Results from evaluating a average gain-model. The top part of the figure shows the estimated, measured and simulated weight. The bottom part of the figure shows the error between estimated and measured soot load in the average gain-model and the internal model. The internal model is the model that is currently used in Volvo cars for estimating soot load. The model can not really capture the characteristics of of the curve for the weighed soot mass, but gives a better estimation than the internal model for any soot mass above 25 grams.

4.2.3   Linear black-box models

Four soot-estimation models based on the black-box models in section 2.4 were designed from the estimation data to fit the measured soot mass. This was done using MATLAB's SYSTEM IDENTIFICATION TOOLBOX, see [6]. For each model estimation, the initial states where chosen as zero. When evaluating different types of estimated models, results have shown that selecting the parameter *focus* to 'simulation' in the toolbox, generally results in models which better predict soot mass. Therefore, this have been used for all estimated models.

Inputs to the models were forward gain, upstream temperature, flow and output was measured soot. The estimation data consisted of multiple series of shorter measurement with varying soot ranges and the validation data of a longer measurement series ranging from 2 to 30 grams soot load.

Choosing the model order

When choosing the order of the models it was taken into account that the confidence intervals for the poles and zeros should not overlap each other. The criteria that each pole/zero Z should fulfill $|Z| \leq 1$ was also kept to prevent the solution from being unstable. For the BJ model flow as an input had to be excluded to create a stable model. The result from the best models when simulating the validation data can be seen in the plots in Figure 4.13. In the figure, the following model parameters where used to obtain the best fit of the simulated mass to the measured mass.

ARX: $n_a = 2$, $n_b = [1\ 1\ 1]$ and $n_k = [1\ 1\ 1]$.

ARMAX: $n_a = 2$, $n_b = [2\ 2\ 2]$, $n_c = 1$ and $n_k = [1\ 1\ 1]$.

OE: $n_b = [2\ 2\ 2]$, $n_f = [1\ 1\ 1]$ and $n_k = [1\ 1\ 1]$

BJ: $n_b = [1\ 1\ 0]$, $n_c = 2$, $n_d = 2$, $n_f = [1\ 1\ 1]$ and $n_k = [1\ 1\ 1]$
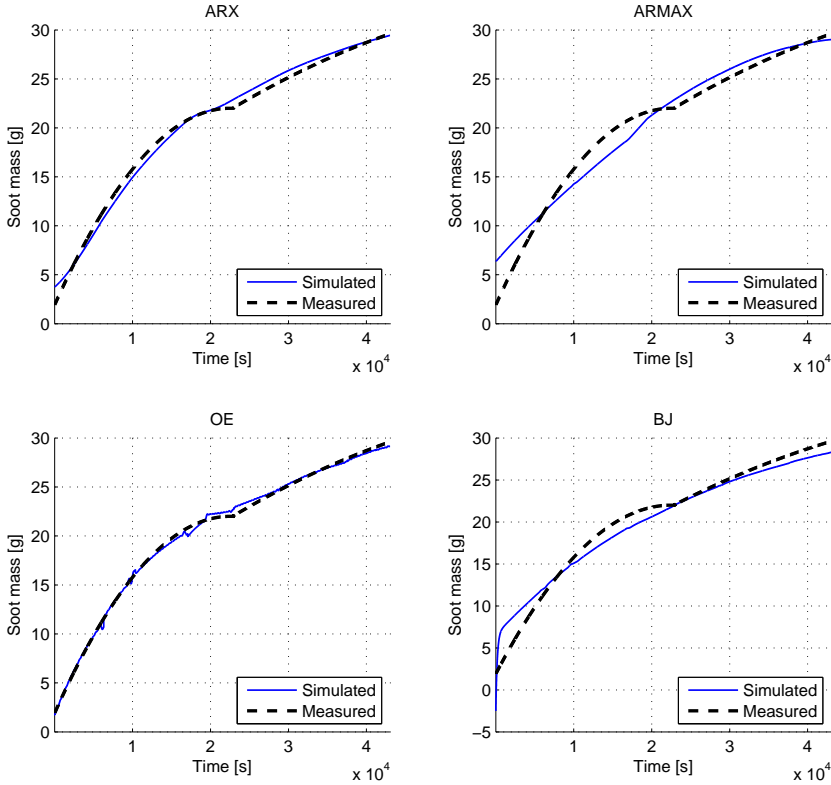

Figure 4.13. Simulated and measured output from the best black-box models. In the figure, the fit of the simulated mass to the measured mass are 91.52%, 80.45%, 95.48% and 81.93% for the ARX, ARMAX, OE and BJ models respectively. The OE has the highest fit and thus is the model which describe the system dynamics best.

As can be seen in Figure 4.13 the OE model yield the best fit around 95% to the measured soot mass. The high fit means that the models describe the true system dynamics well. When computing the fits above, both input and output data was used to compute the initial states for each model to get the best possible fit. This is however not possible when the real mass is unknown, therefore two ways of choosing the initial states are described next.

Choosing initial states x_0

The lack of physical interpretation of the states in the models creates a problem when simulating without knowing the real soot mass since the initial states x_0 can not be computed for the models. According to [17] this is a known problem when there is no information about the model at time $-\infty < t < 0$.

One approach is to set all initial states to zero, see [17]. The model which yield the best prediction when simulating were the OE model. A Simulation for the OE model with all initial states x_0 set to zero can be seen in Figure 4.14. The fit is not as satisfying as when x_0 is estimated but the model still predicts the output quite well. The highest prediction error is about 5 grams.
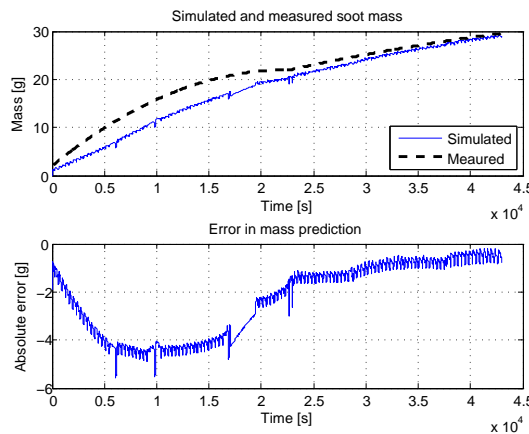

Figure 4.14. The upper plot shows simulated and measured output from the OE model on validation data with all initial states x_0 set to zero. The prediction is not as good as when estimating the initial values from the measured mass. In the lower plot show the absolute error of the simulation compared to the real measured soot mass. As can be seen in the figure the prediction is better when the soot load is high.

Reducing the number of model states

An alternative approach would be to chose models with only one state. All of the previously described black-box models can be described in state space form as

$$\dot{x} = Ax + BU$$
$$y = Cx + DU \tag{4.1}$$

where x are the states, U are the input signals, y is the model output and A, B, C, D are matrices defining the relationships.

If the C matrix equals 1 and the D matrix equals 0 for a model with only one state, this state could be interpreted as the soot mass state. This would allow the model to start simulation from any initial soot mass, but at the cost of lower degrees of freedom for the models and therefore also the ability to capture the true dynamics of the system.

A reduced ARX model was developed with only one state for comparison. The fit for the reduced ARX model with estimated initial state can be seen in Figure 4.15 and the simulated output when setting the state to the real initial soot mass can be seen in Figure 4.16.

The results when simulating shows that the reduced ARX model with its initial state set to the true soot mass, shows better prediction in soot mass than the other models with multiple states, when all initial states are set to zero. Even though the OE model had the best fit and showed a good prediction when simulating, the reduced ARX model still show less error in prediction since the initial state can be set to the true mass.
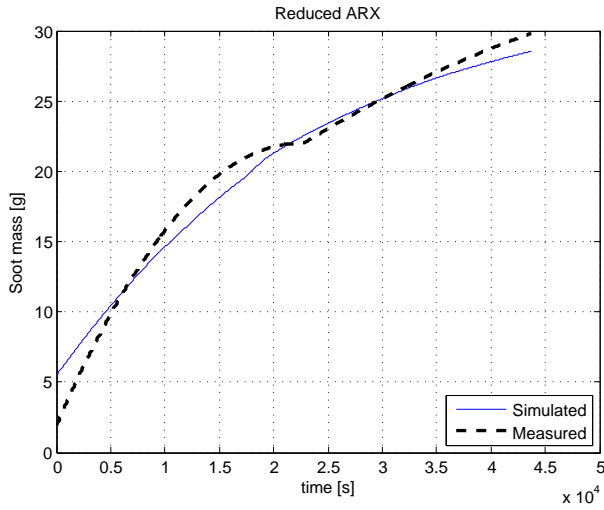
Figure 4.15. Simulated and measured output from the reduced ARX model with only one state. The parameters chosen as $n_a = 1$ $n_b = [1\ 1\ 1]$ and $n_k = [1\ 1\ 1]$. The fit of the simulated mass to the measured mass is 84.62%
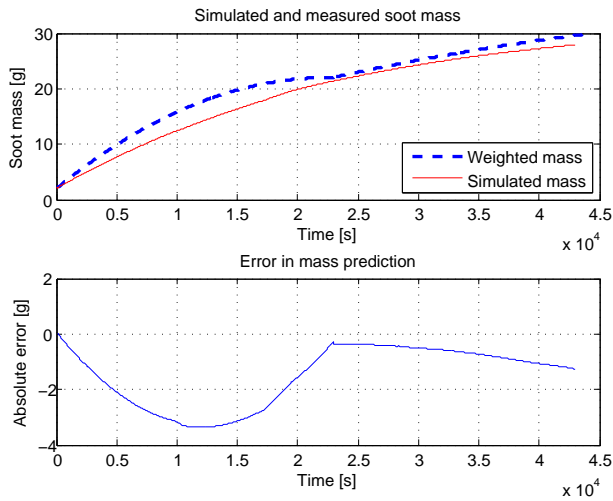

Figure 4.16. The upper plot shows the simulated and measured output from the reduced ARX model on validation data with only one initial state, mass, set to the real initial soot mass 2 grams. The lower plot shows the absolute error of the simulation compared to the real measured soot mass. The reduced ARX model yields less error in the beginning, but deviates more at higher soot loads compared to the OE model with initial states set to zero.

Chapter 5

Model evaluation

In this chapter, a sensitivity analysis of the estimated models is performed. Also, other factors which could affect the performance of the soot estimation are discussed.

5.1 Sensitivity analysis

A sensitivity analysis is performed for each of the four black-box models in section 4.2.3 and the average gain-model in section 4.2.2. The analysis is performed by first adding a bias error and then Gaussian noise to each of the input signal, one signal at a time and then analyze the effects on the estimated soot mass. As bias error the following values were used for each input; gain $+2$ dB, temperature $+20$ °C and flow $+20$ m^3/h. The relative errors in Figures 5.1-5.3 and Figures A.1-A.5 in Appendix A are computed as

$$Relative\ Error = 100 \cdot (P_{NF} - P_{BE})/P_{NF} \tag{5.1}$$

where P_{NF} is the prediction without error and P_{BE} is the prediction with a bias error.

It is highly desirable that the chosen model has the ability to suppress the effect from bias errors in the input signals, especially the forward gain. All the models estimates the soot mass mainly based on the forward gain signal, and uses upstream temperature and flow to improve the estimation further. The model of choice should have a relative error which decreases, or at least settles with increased soot mass, to prevent the simulated soot mass from drifting away to far from the 'true prediction'. A relative error which settles at a certain value can be back-traced to a specific uncertainty; a certain percentage of the output error can be described with an absolute bias error in the input signal.

5.1.1 Average gain-model

The average gain-model output was computed with a Matlab script using matrices multiplication. A bias error was then added to the three input signals one at a time and the results can be seen in Figures 5.1-5.3. The average gain-model is very sensitive to changes in the average gain signal while it is not that sensitive to an error in the flow or temperature measurements. The high sensitivity to bias error in the forward gain signal is undesirable as described in previous section.
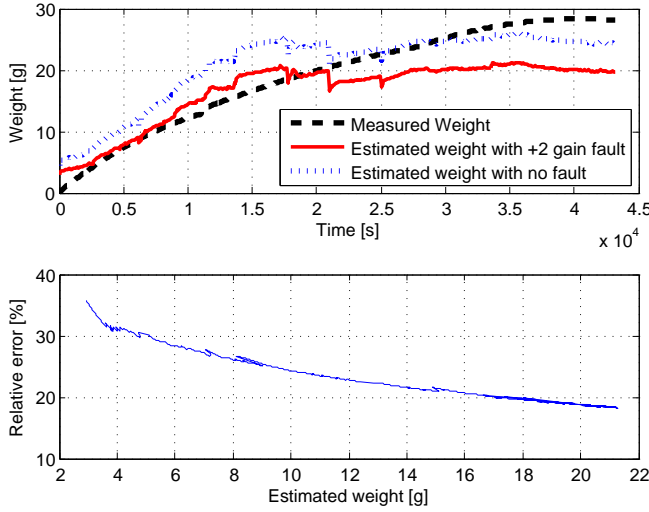

Figure 5.1. The effects on the average gain-model when a bias error of 2 dB is added to the gain input signal. The upper plot shows the estimated soot load with and without a bias error as well as the measured soot weight. The lower plot shows the relative error. The high sensitivity to bias error in the forward gain signal is undesirable
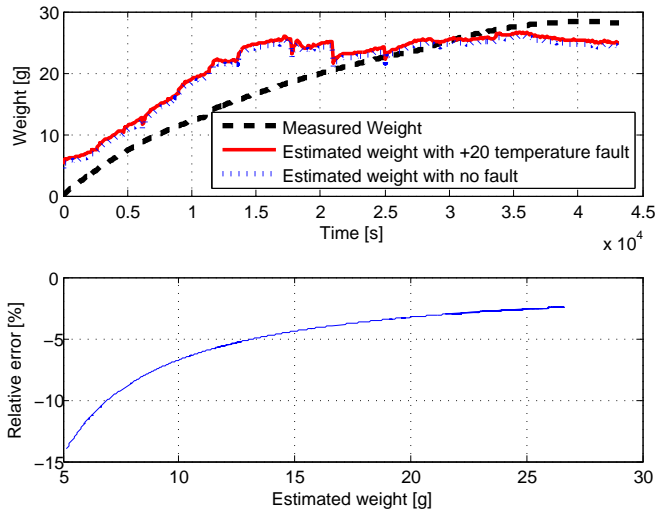
Figure 5.2. The effects on the average gain-model when a bias error of 20 °C is added to the temperature input signal. The upper figure shows the estimated soot load with and without a bias error as well as the measured soot weight. The lower figure shows the relative error. The sensitivity to temperature is low which is desirable.
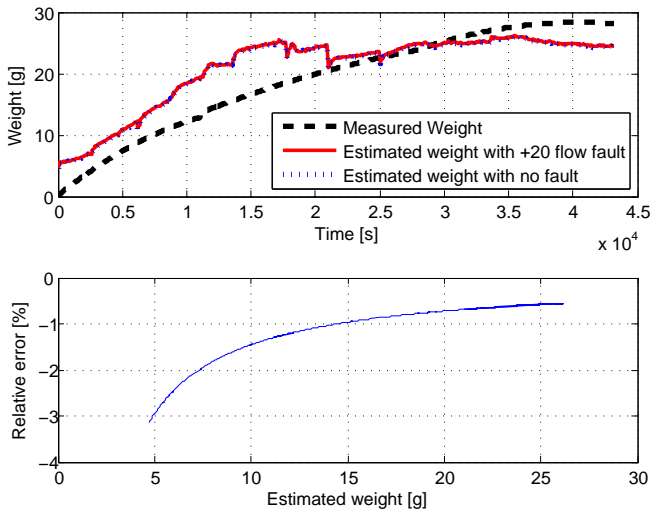

Figure 5.3. The effects on the average gain-model when a bias error of 20 m³/h is added to the flow rate input signal. The upper figure shows the estimated soot load with and without a bias error as well as the measured soot weight. The lower figure shows the relative error. The sensitivity to flow is low which is desirable.

5.1.2 Black-box models

A SIMULINK model was constructed for simulating and adding bias errors and noise to the input signals for the black-box models. The SIMULINK model can be seen in Figure 5.4.

In the following subsections, the result on how the output signal is affected when introducing a bias error on each of the input signals for each black-box model is presented. For the forward gain measurements, a bias error of 2 dB was added. For temperature and flow measurements bias errors of 20 °C and 20 m^3/h was added. A summary of the results from the bias error simulation can be seen in Table 5.1. The simulation output when introducing the bias errors to the input signals can be seen in Appendix A, Figures A.1-A.5. Three of these models are also shown in Figures 5.5-5.7.
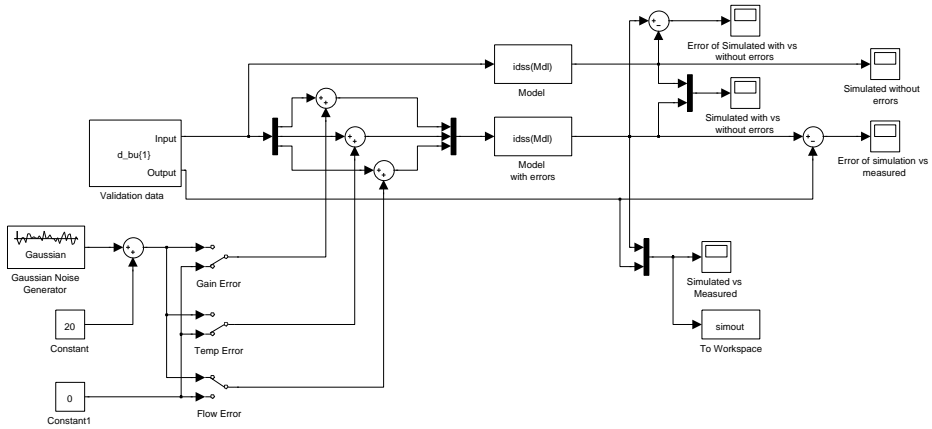

Figure 5.4. A SIMULINK model for simulating the linear black-box models. Noise and bias errors can be added to each input signal.

ARX-model

The ARX model is quite sensitive to changes in both gain, flow and temperature. The relative error increases with soot load. An increase in the relative error is undesirable since observations have shown that the coaxial connectors are a great uncertainty affecting the gain signal. The prediction from the ARX model for the bias errors can be seen in Figure 5.5.

Reduced ARX-model

The reduced ARX model is not as sensitive to a bias error as the regular ARX. The relative errors are small and settles with increased soot. The prediction from the reduced ARX model for the bias error can be seen in Figure 5.6.

ARMAX-model

The ARMAX model shows a highly undesired response to bias errors in gain, flow and temperature measurements. The relative error when introducing a bias offset seem to deviate from the 'true prediction' somewhat exponentially with increasing soot mass. The soot prediction is still stable though but is drifting away from the 'true prediction'. The prediction from the ARMAX model for the bias error is shown in Figure A.3. The relative error increases with higher soot mass for all bias error in the input signals. This can also be seen in the simulation plot where the estimations with errors deviates from the estimations without errors.

OE-model

The OE model is mostly sensitive to bias errors in temperature. The relative error settles for all inputs with a bias error. The prediction from the OE model for the bias error is shown in Figure 5.7.

BJ-model

The BJ model shows a decaying relative error for a bias offset in gain, which is highly desirable. The relative error settles with increased soot mass. Since the flow input had to be excluded as an input to generate a stable model, the flow dependence is zero. The prediction from the BJ model for the bias error is shown in Figure A.5.

Table 5.1. Summary of the bias offset sensitivity.

Model		Relative error		Relative error at 30g
	Gain	Increasing		20%
ARX	Temperature	Increasing		32%
	Flow	Increasing		-17%
	Gain	Stabilizing		-1.7%
Reduced ARX	Temperature	Stabilizing		3.4%
	Flow	Stabilizing		1.5%
	Gain	Increasing		-27%
ARMAX	Temperature	Increasing		-28%
	Flow	Increasing		22%
	Gain	Decreasing		-7%
OE	Temperature	Decreasing		-4.8%
	Flow	Increasing		7.5%
	Gain	Stabilizing		-0.75%
BJ	Temperature	Stabilizing		5.2%
	Flow	Stabilizing		0%

The table shows the relative error behavior when introducing a bias error on the input signals; 2 dB added to the gain, 20 °C added to the temperature and 20 m^3/h added to the flow. The first column is the model and the second is the input signal to which the bias error is added. The third column is how the relative error behaves as soot load is increasing. The last column shows the relative error at 30 grams soot load.
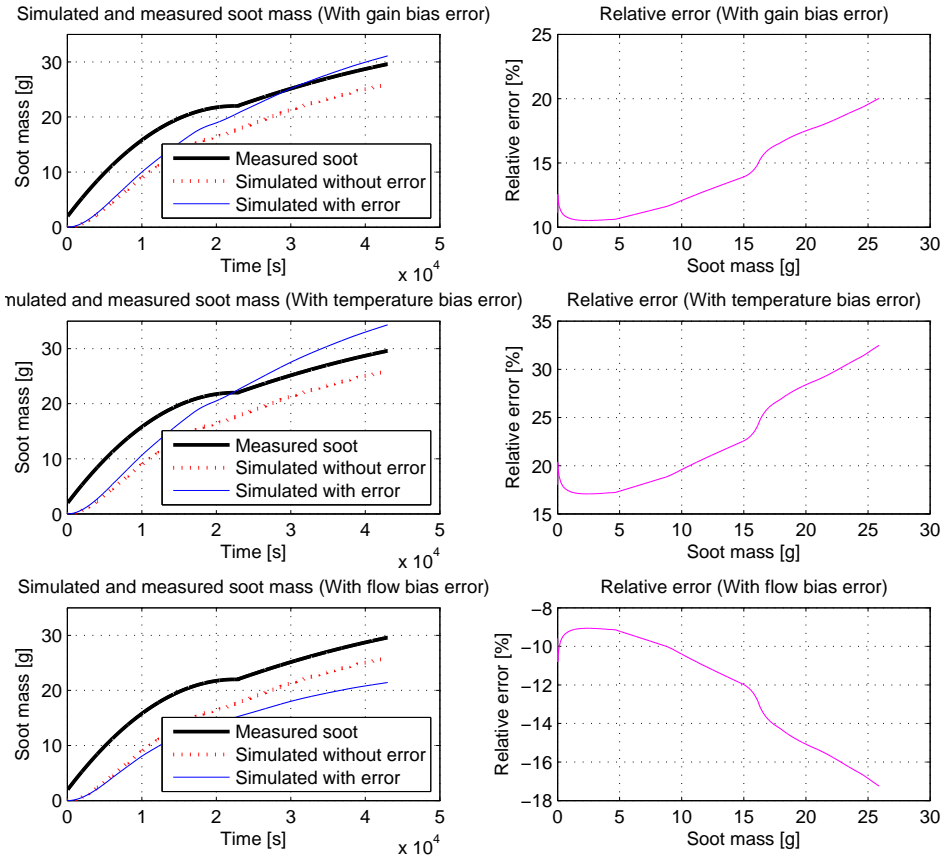
Figure 5.5. The effect on the ARX model when a bias error of 2 dB on the gain, 20 °C on the temperature and 20 m^3/h on the flow are added to the input signals, one at a time. Each row corresponds to a bias error for gain, temp and flow respectively. The left column is prediction with and without error compared to the weighed mass. The right column is the relative error for the prediction with the bias error compared to the prediction without error. The relative error increases with increased soot mass for all bias errors in the input signals.
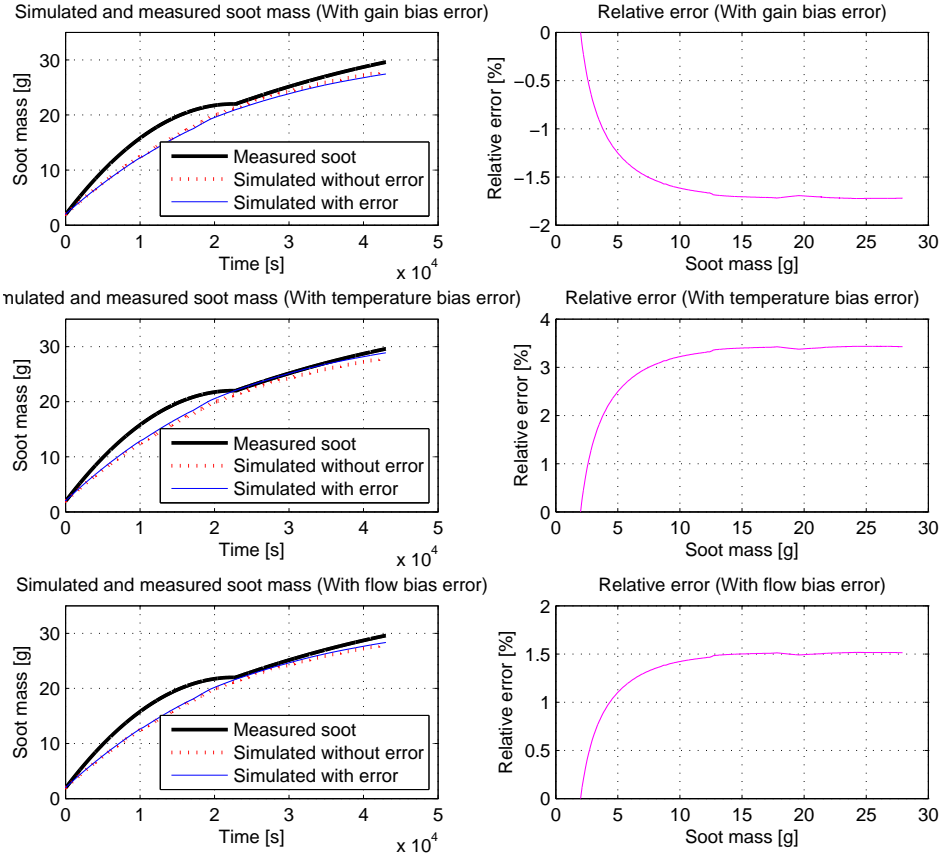
Figure 5.6. The effect on the reduced ARX model (only one state) when a bias error of 2 dB on the gain, 20 °C on the temperature and 20 m³/h on the flow are added to the input signals, one at a time. Each row corresponds to a bias error for gain, temp and flow respectively. The left column is prediction with and without error compared to the weighed mass. The right column is the relative error for the prediction with the bias error compared to the prediction without error. The relative error stabilizes for all bias errors on the input signals.
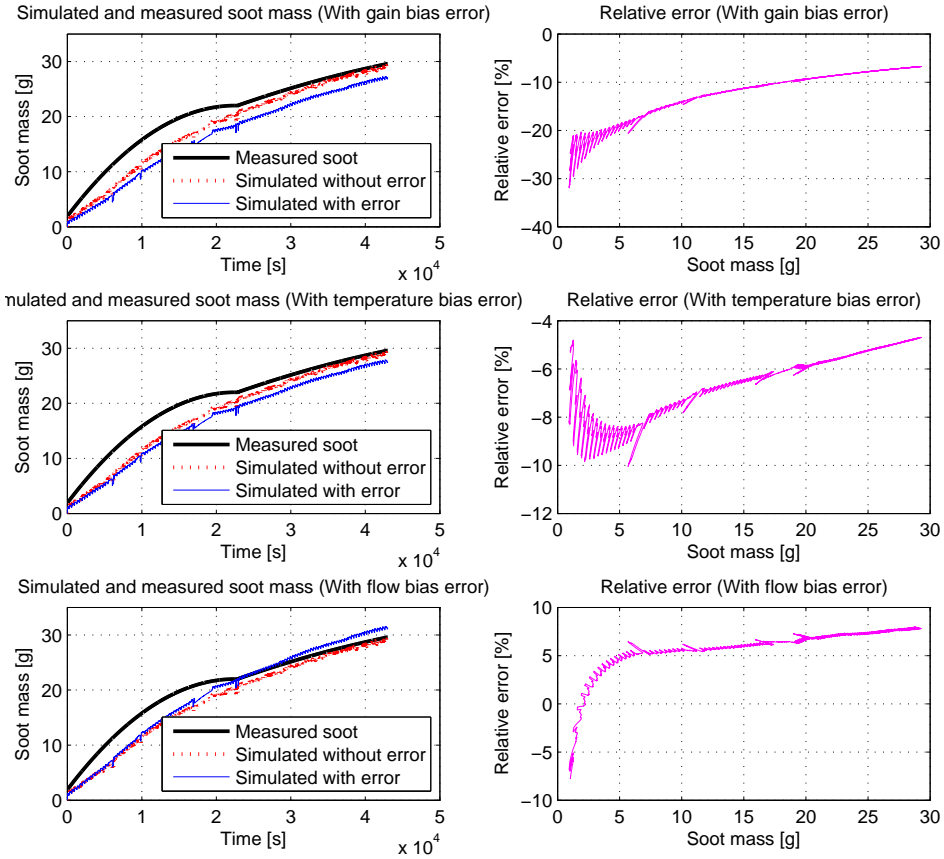
Figure 5.7. The effect on the OE model when a bias error of 2 dB on the gain, 20 °C on the temperature and 20 m^3/h on the flow are added to the input signals, one at a time. Each row corresponds to a bias error for gain, temp and flow respectively. The left column is prediction with and without error compared to the weighed mass. The right column is the relative error for the prediction with the bias error compared to the prediction without error. The relative error decreases with increased soot mass for bias errors in gain and temperature but increases for a bias error in the flow.

To evaluate how sensitive the models are to disturbances in the input signals, the models were simulated by adding an additive Gaussian noise to each of the input signals respectively. The noise had a mean value of zero and a variance of 10. The output from simulating without disturbances was subtracted from the simulation with noise, thus only showing the influence in the output signal caused by the noise. The resulting output from the models are shown in Figures A.6 - A.10. For comparison the results from the reduced ARX and the OE model can be seen in Figures 5.8-5.9. The variance for the noise is much higher than expected for the forward gain in the true system but still shows the gain factor of the noise from input to output.
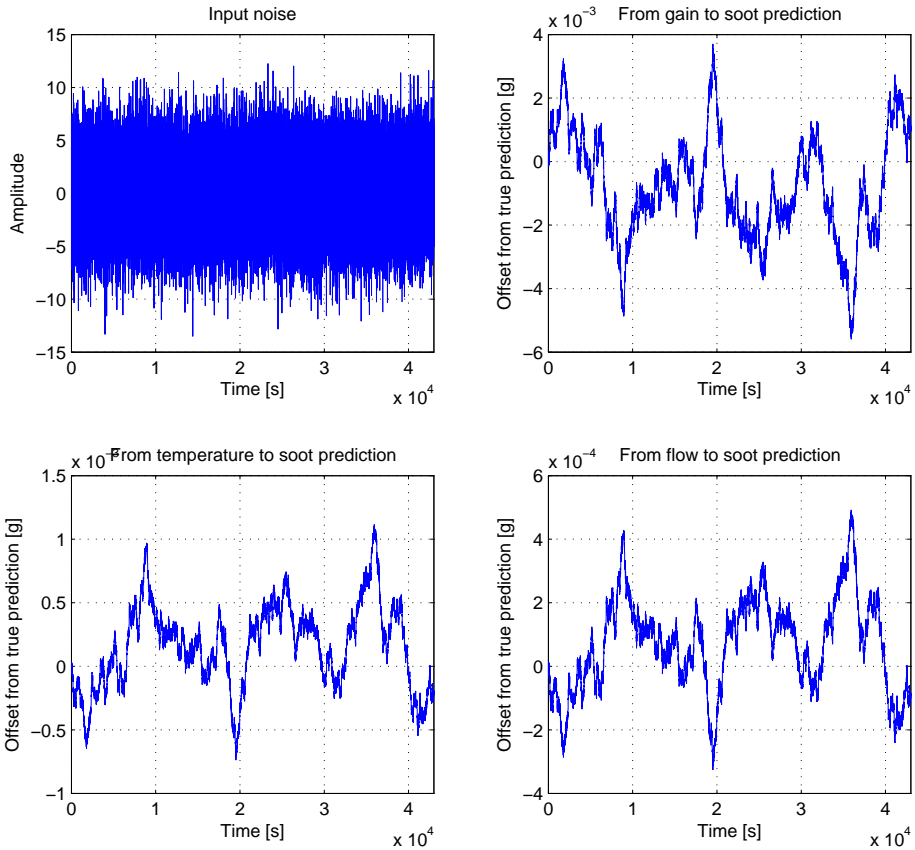

Figure 5.8. The effect on the output for the reduced ARX model when Gaussian noise, with mean value zero and variance 10, is added to each of the three input signals; gain, upstream temperature and flow, one at a time. In the figure the output from the simulation without noise is subtracted from the output from simulation with noise, thus only the output from the noise is shown. Top left: input noise, top right: noise added to the gain signal, bottom left: noise added to the temperature signal, bottom right: noise added to the flow signal.

Figure 5.9. The effect on the output for the OE model when Gaussian noise, with mean value zero and variance 10, is added to each of the three input signals; gain, upstream temperature and flow, one at a time. In the figure the output from the simulation without noise is subtracted from the output from simulation with noise, thus only the output from the noise is shown. Top left: input noise, top right: noise added to the gain signal, bottom left: noise added to the temperature signal, bottom right: noise added to the flow signal.
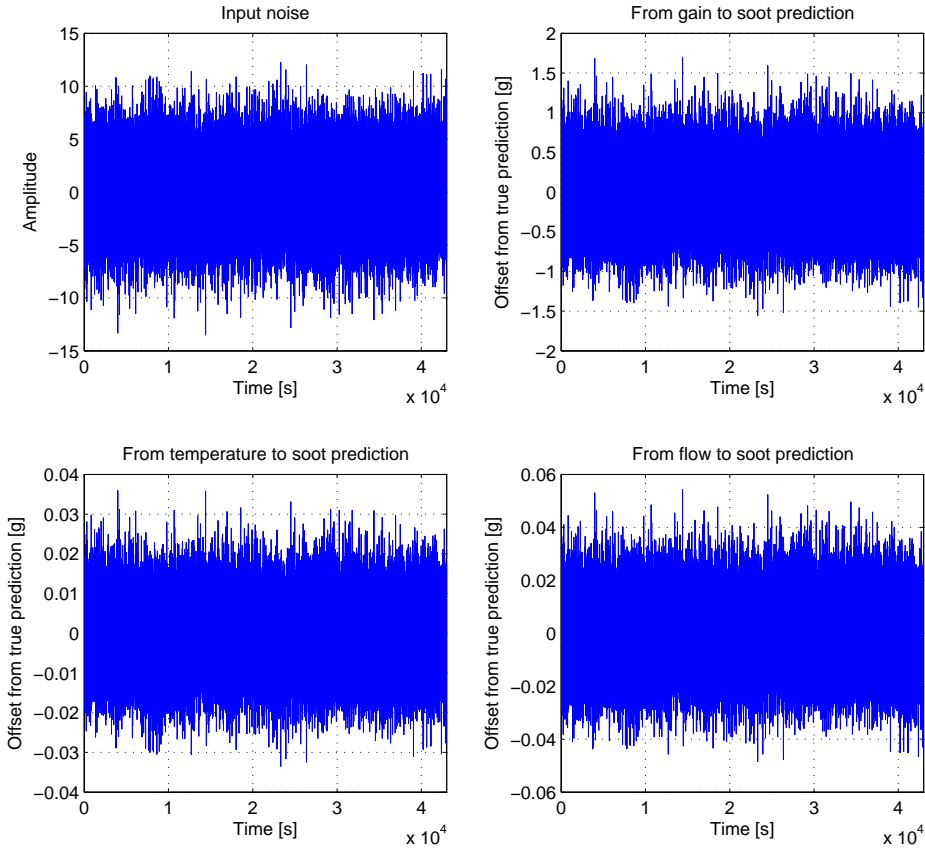
Both the ARX and ARMAX model show strong sensitivity to bias errors in all input signals, which is highly undesirable. It can be seen in Figure 5.6 that the reduced ARX model is not nearly as sensitive to bias errors as the regular ARX model, see Figure 5.5 for comparison.

The reduced ARX, OE, and the BJ model show less influence from bias errors. Of these models, the BJ model shows the least sensitivity to bias errors in the gain signal and relatively low sensitivity to bias errors in temperature. The OE model has higher sensitivity to bias errors compared to both the BJ and the reduced ARX model. The reduced ARX model is not very sensitive to bias errors and

shows low relative errors for all signals.

All models show high suppressing properties towards noise in the input signals. Only low frequency disturbances passes through most of the models and the influence on the soot estimation for these frequencies are negligible. One observation is that the OE model does not yield as good noise suppressing for the gain as the other models.

The OE model dampens the input noise amplitude by a factor 10. The soot prediction error for the OE model, caused by noise in the forward gain signal, will therefore have an amplitude of 10% of the input noise amplitude. Considering that the true system has not shown nearly as high noise variance for the forward gain, this is still a good suppression of noise. By computing the variance for two consecutive measurement series from the soot sensor, it shows a variance of approximately 0.75. This means that the prediction error caused by the true noise will be approximately ± 0.075 grams.

5.2 Factors disturbing estimation

When gathering data measurements from the system, there is a number off different uncertainties for each measured signal. Removing and attaching sensors when weighing also affect the sensor output. In this section some relevant factors will be discussed.

5.2.1 Forward gain

The soot sensor's antennas and its coaxial cable connectors have been shown to have a relatively large impact on the measured signal when disconnected and reconnected again. The initial measurements on the DPF disconnected to the car showed an offset in gain up to 1.6 dB, see Figure 5.10. Up to 2.5 dB offset has been seen in measured data, see Figure 5.11. The forward gain ranges from approximately -20 dB for no soot load to -30 dB for 30 grams of soot load, so an offset of 2.5 dB is quite large in comparison to the operating range which is only four times as wide.
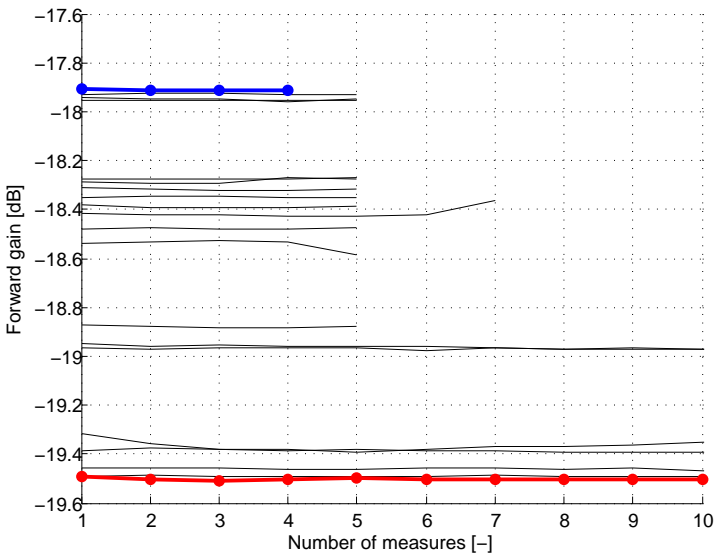
Figure 5.10. The offset for the forward gain for an empty filter caused by removing and reconnecting the coaxial cables and antennas. Each horizontal line is a measure and prior to each measure the coaxial cables where removed and reattached again. The highest and lowest damping differs about 1.6 dB for the empty filter.
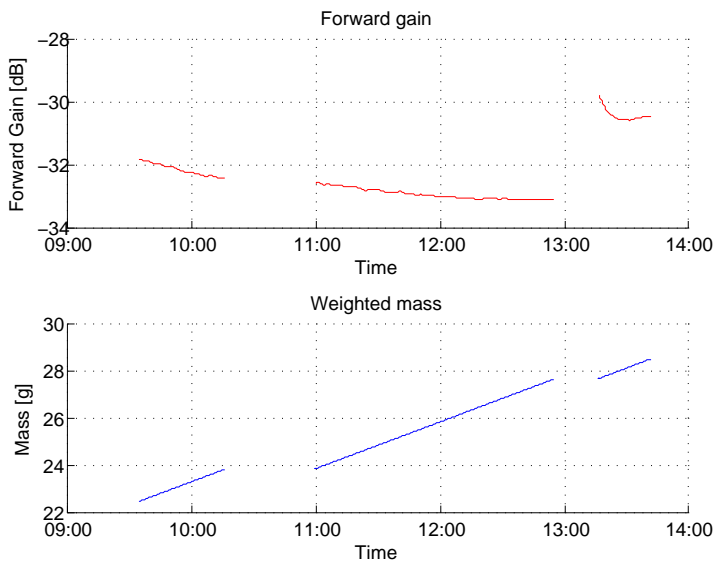

Figure 5.11. The offset of the forward gain caused by removing and reconnecting the coaxial cables and the antennas. In the figure three measurements and two weighings are shown. Weighing occurs at about 10:30 and 13:00. The forward gain before and after weighing at 13:00 shows an offset of 2.5 dB.

5.2.2 Weighing of soot mass

The scale used for weighing the soot mass had an accuracy of 0.1 gram for masses up to 3 kg and an accuracy of 1 gram for masses between 3 kg and 20 kg. The method of choice for measuring the soot mass was differential weighing of the whole DPF. An empty DPF with no soot weighs 8102 grams, therefore the accuracy of the scale is whole grams only. A measured soot mass can therefore differ ± 0.5 grams from the true value. A reference weight of 8210 grams was weighed before each measurement to ensure the validity for each weighing (i.e. making sure the scale does not drift).

5.2.3 Temperature

The measured temperature used in the estimations is the temperature upstream of the DPF, see element 4 in Figure 2.1. The position of the temperature sensor is not exactly the same as the RF-antenna and therefore the temperature of the soot sensor may differ a bit from that of the temperature sensor.

5.2.4 Flow rate

The flow rate through the DPF used in the models is a computed value based on the engine speed and flow rate of air and fuel into the cylinder. The uncertainties in the computed flow rate is unknown but it is used for calibration of other models in the system.

5.2.5 Soot accumulating on the antenna

Heavy soot accumulation on the upstream sensor has been observed. How this affects the measurements is unknown but it could be an explanation to why the average gain is so high after a regeneration to half full DPF, see Figure 4.5.

Chapter 6

Method for soot estimation

In this chapter the developed method for soot estimation is presented. The choice of model, how to minimize the uncertainties when collecting data for estimation, how to minimize errors in the prediction as well as advantages and drawbacks with the developed method will be discussed.

6.1 Choice of model structure

Each of the evaluated models structures in section 4.2 have different advantages and disadvantages when compared to each other. The average gain-model is the only model which has the ability to start the estimation from an unknown soot mass. The soot prediction from this model however is not as good as the black-box models when the soot load is higher than 20 grams.

For the linear black-box models, the OE and reduced ARX models have the best soot mass prediction with an absolute error of ± 4 grams when used for soot loads from 0 to 30 grams. When taking into account the sensitivity analysis, see section 5.1, the reduced ARX model is to prefer. The reduced ARX model is not as sensitive to bias errors compared to the OE model and better at suppressing noise in the measured input signals. Therefore, the proposed model for estimating soot mass is a reduced ARX model.

Since the reduced ARX model only has one state which could be interpreted as the soot mass, the simulation may start from any known soot mass by setting the initial state to the known mass. If the soot mass is unknown the DPF needs to be regenerated to zero before use. If there is a need to estimate the soot load at an unknown mass, use the average gain-model to get a rough estimate.

The reduced ARX model gives the best prediction for this particular DPF. If the soot sensor is to be used with another type of DPF (i.e. different shape, filter substrate), any of the other model structures may yield better soot prediction and must therefore be evaluated.

6.2 Collecting the estimation data

Good estimation data is a key factor when estimating a model. The estimation data should consist of different driving cycles, making sure as much information as possible of the soot sensor's dynamics is present in the estimation data. Both slow and faster soot build up cycles should be included in the estimation data. Soot sensor output, flow rate through the DPF and temperature upstream of the DPF should be logged. Weighings of the DPF should be made, which are later used as the output when estimating the models.

The driving cycles should be designed to include changes in the flow and the temperature which corresponds to their respective operating range in a car.

Regenerations should be performed for a longer time than nominal, thus making sure the soot mass is close to zero. Automatic regeneration in a car is stopped when the internal model reaches below a certain threshold. When collecting estimation data, the regeneration should be forced for a longer time to make sure as much soot as possible is burnt out.

6.2.1 Minimizing uncertainty during soot mass estimation

The coaxial cables have shown to be the biggest uncertainty when removed and reconnected, see section 5.2.1. When collecting the estimation data, focus should lie on minimizing the uncertainty from the cable connectors. Minimizing this uncertainty can be achieved in two ways, either by using a reference level or by weighing the complete soot sensor apparatus, which are both described next.

Adjusting measurements to a reference level

By setting a reference level for the forward gain in an empty filter, gathered data can be adjusted manually to compensate for offsets in the forward gain caused by removing and reattaching the cables. For each measurement starting from zero, the forward gain should be adjusted to the set reference level. During the soot build up process, weighing of the filter may cause an offset in the forward gain caused by the cables. Any offsets should be adjusted manually to fit the global curve trend defined by the first measurement.

In Figure 6.1, an example is shown where the upper plot shows a typical behavior for two sequent measurements with a weighing in between them. At the beginning of the second measurement the temperature reduction (caused by DPF cooling when weighing) cause an increase in forward gain which decays after approximately 2500 seconds. Note that the measurements in the figures are fictional and the time is not that of the true system. The second measurement is however still offset by approximately 2 dB compared to what would be expected when looking at the trend of the first measurement. In the lower plot in the same figure, the second measurement has been manually adjusted to a trend, defined by looking at the first measurement. The trend can be estimated and following measurements

can be adjusted to the trend using, e.g., least squares described in section 2.3.
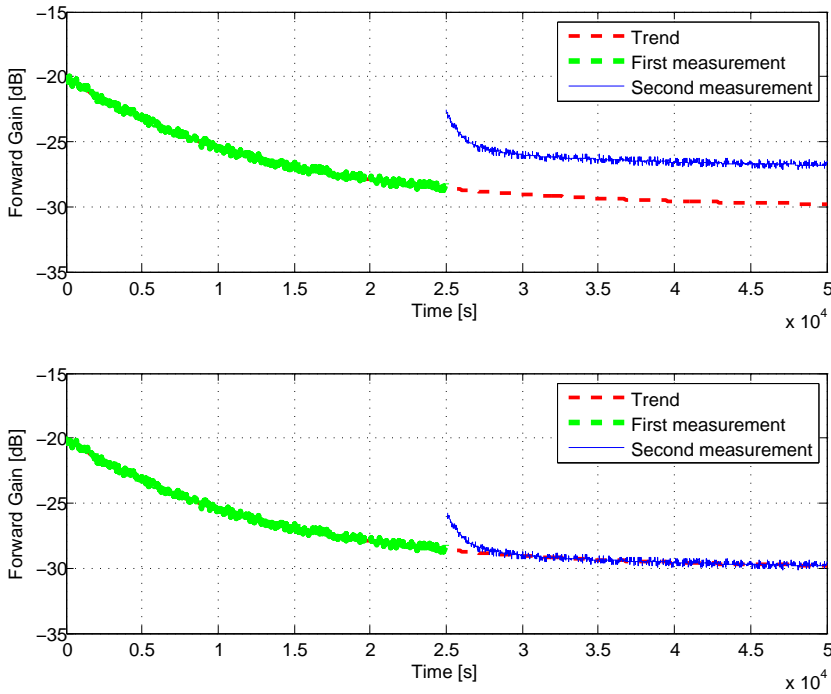

Figure 6.1. The upper plot shows simulated data representing a typical behavior when weighing between two measurements. In the lower plot the second measurement has been adjusted to the trend line of the first measurement.

The approach of using a reference level and adjusting other measurements to fit a trend, can be difficult to use if the trend is hard to identify. However is has been observed in the measurements that a trend usually can be identified for some of the longer measurements. In Figure 5.11, a trend can easily be seen for the first two measurements. In the figure, the increase in forward gain, caused by the lower temperature after weighing, has been removed in the pre-treatment of the data, see section 4.2.1. The third measurement is too short to be properly fitted to the previous data due to Excel communication problem.

Weighing the complete sensor apparatus

An alternative way to minimize the uncertainty caused by the cables, is to include the sensor cables and sensor control box when weighing the DPF. By not removing the cable connectors, the offset in forward gain caused by the cables will be eliminated. When the sensor is installed in a car this is a complicated task, considering

that the cables are usually passed through the insulation of the car door to be able to use the computer in the coupe. Weighing of the complete apparatus is more usable in a test cell where the sensor and the sensor box is well exposed and can be removed easily.

6.3   Estimating of the model

When the estimation data has been gathered, and the uncertainty caused by the coaxial cables has been minimized, the data may be pre-processed in order to achieve a better model estimation, see section 4.2.1. A reduced ARX model can be estimated using e.g. SYSTEM IDENTIFICATION TOOLBOX, which is a separate toolbox for MATLAB. When estimating the model, temperature, flow and the average forward gain are used as inputs and the weighed soot is used as the output signal.

6.4   Minimizing error in prediction

When using the developed reduced ARX model for estimating the soot load, it is important to keep in mind that it is only valid for the soot range in which the model is estimated for. If the model is estimated with estimation data between 0 and 25 grams, the model can not be guaranteed to work above 25 grams of soot load. As can be read in section 4.1.5, soot distribution is a limitation when using the sensor. Partial regenerations should therefore be avoided to receive a better prediction.

It can be difficult to know the exact soot mass in the DPF when starting a new experiment, and since the initial soot mass must be known in order to use the reduced ARX model it is recommended to force a full regeneration of the DPF using the same method as when collecting the estimation data, thus making sure the soot mass is close to zero.

When using the model on a cold DPF, the engine must reach its operating temperature before the prediction can be considered valid due to the temperature dependence of the sensor.

The problem with the coaxial cables offset previously described will not affect the soot prediction when using the model since the cables are not removed except when weighing, which is not done when the model is in use.

Chapter 7

Conclusions

In this chapter the conclusions drawn from the performed work are presented. This chapter also contains future work.

7.1   Conclusion

A method for soot estimation using General Electric's Accusolve soot sensor that is based on radio frequency technology has been developed. Series of measurements have been performed in both a test cell and a Volvo passenger car. These measurements have been used to estimate and validate a model using the developed method.

Parameters that have been shown to affect the measurements are: temperature in the DPF, flow rate through the DPF, positioning of the antennas and distribution of soot in the filter. The temperature and flow rate can be used as inputs to the model and therefore be compensated for to improve the estimation.

The linear black box models show better stability and less absolute error in prediction compared to the average gain-model. All linear black box models except the reduced ARX model requires that the initial soot mass is zero to be able to make a good prediction. The reduced ARX model may start from any known soot mass but does not describe the system dynamics as well as the other linear black box models. The OE model describes the system dynamics best, but due to the lack of physical interpretation the initial states can not be estimated good enough to make use of the good system description, see section 4.2.3. The average gain-model is unaffected by the starting conditions and therefore the model may be used as a rough estimate at unknown initial soot masses.

Based on the analyses, the conclusion is that the model of choice should be the reduced ARX, which show good resistance to bias error as well as to suppressing noise in the input signals. The absolute prediction error for the reduced ARX is less than 4 grams when used for soot prediction from 0 to 30 grams.

The coaxial cables have shown large uncertainties concerning the forward gain; when removed and reconnected again the gain may be offset, see section 5.2.1. This uncertainty can be minimized using one of the two methods described in section 6.2.1.

7.2 Future work

In this section some suggestions of future work which would improve the developed models even further are proposed.

Regeneration model

To further improve the usability of the developed method for soot estimation described in Chapter 6, it may be possible to include regenerations in the current model, or by developing a separate model which handles regenerations only. Not enough data was collected to generate a regeneration model in thesis. Developing a model including regenerations will require that a wider range of temperatures is used for estimating the model.

Observations have shown that during regeneration the soot distribution differs from that of regular soot build up, therefore a more extended series of tests must be performed for regeneration to be able to evaluate the possibility to create a model for regenerations.

Soot distribution

The soot sensor's dependency of soot distribution is something that needs to be investigated further. This thesis only covers two different types of distributions and there is currently no method for measuring the soot distribution in the filter at Volvo today. It would be of interest to combine the soot sensor with a system or method for measuring the soot distribution in the filter.

Coaxial cables

During the work the coaxial cable connectors were the main problem when developing a model to estimate soot mass. The sensor output may have an offset when the cables are removed and connected again compared to the measurements before. If the current sensor is to be used for soot estimation, the recommendation is to test if it is possible to weigh the DPF without disconnecting the coaxial cables, the GE sensor apparatus will then need to be weighed since the coaxial cables are attached to the sensor micro controller. This will probably solve the problem when developing a model but will still be a problem since a new model needs to be developed each time the sensors are disconnected or replaced when used in another car.

Appendix A

Simulation outputs

In this appendix the figures from the sensitivity analysis in section 5.1 are presented. The figures include results from the bias and noise error analysis for the linear black box models.
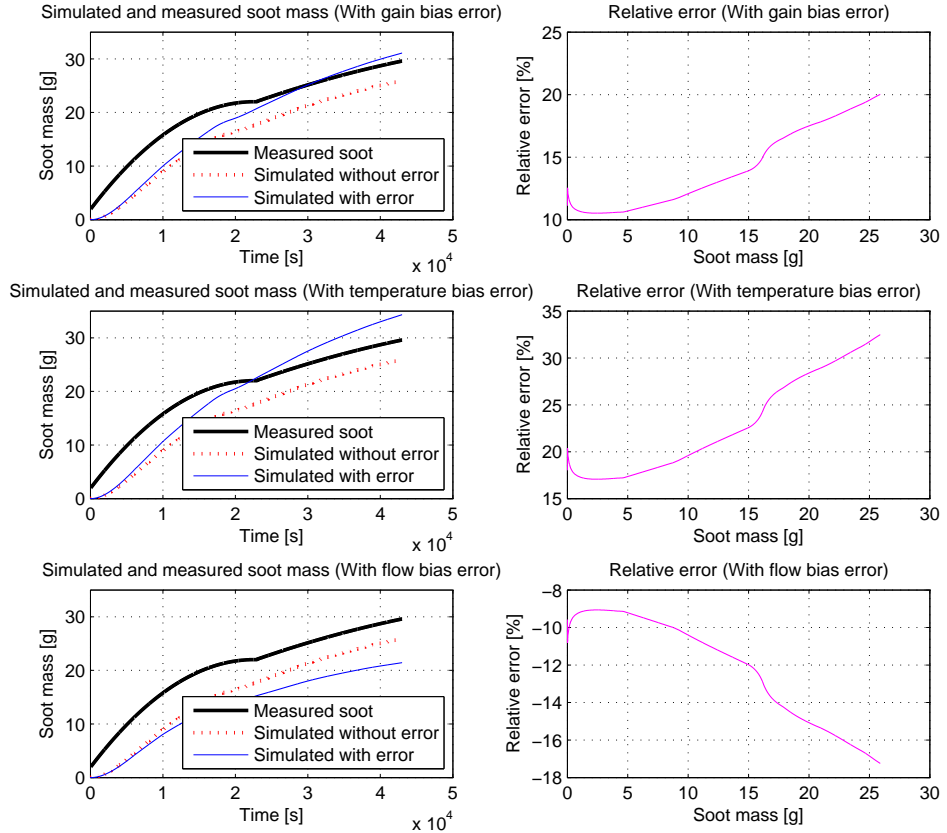
Figure A.1. The effect on the ARX model with a bias error of 2 dB on the gain, 20 °C on the temperature and 20 m^3/h on the flow input signals, one at a time. Each row corresponds to a bias error for gain, temp and flow respectively. The left column is prediction with and without error compared to the weighted mass. The right column is the relative error for the prediction with the bias error compared to the prediction without error. The relative error increases with increased soot mass for all bias errors in the input signals.
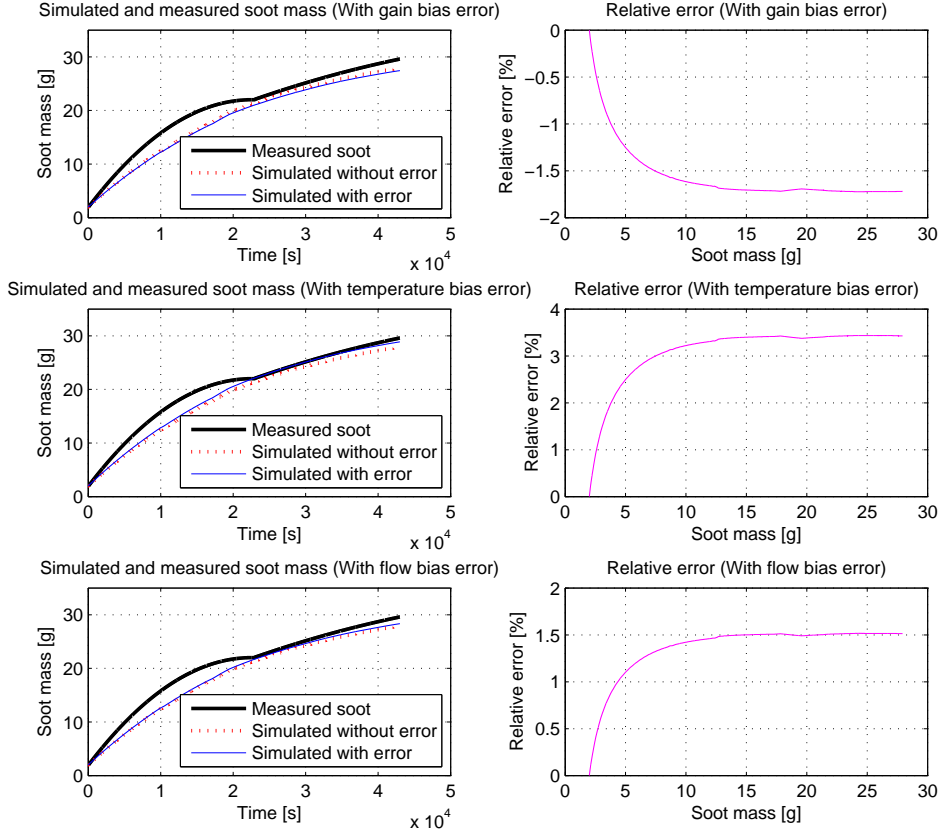
Figure A.2. The effect on the reduced ARX model (only one state) with a bias error of 2 dB on the gain, 20 °C on the temperature and 20 m^3/h on the flow input signals, one at a time. Each row corresponds to a bias error for gain, temp and flow respectively. The left column is prediction with and without error compared to the weighted mass. The right column is the relative error for the prediction with the bias error compared to the prediction without error. The relative error stabilizes for all bias errors on the input signals.
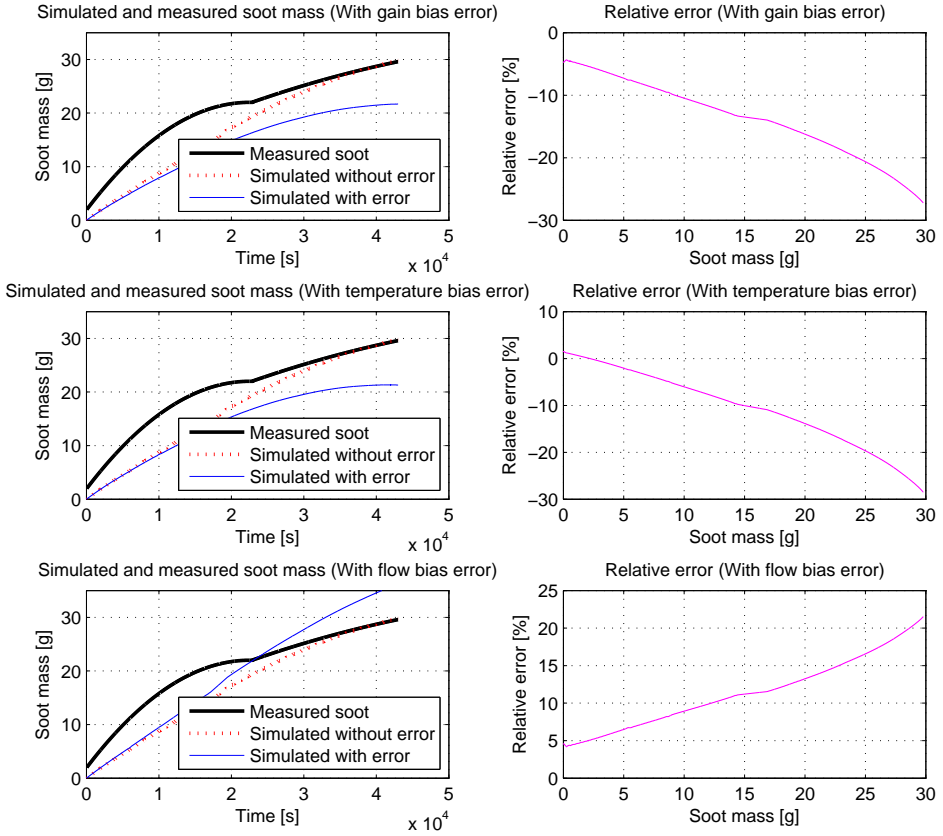
Figure A.3. The effect on the ARMAX model with a bias error of 2 dB on the gain, 20 °C on the temperature and 20 m³/h on the flow input signals, one at a time. Each row corresponds to a bias error for gain, temp and flow respectively. The left column is prediction with and without error compared to the weighted mass. The right column is the relative error for the prediction with the bias error compared to the prediction without error. The relative error increases with increased soot mass for all bias errors in the input signals.
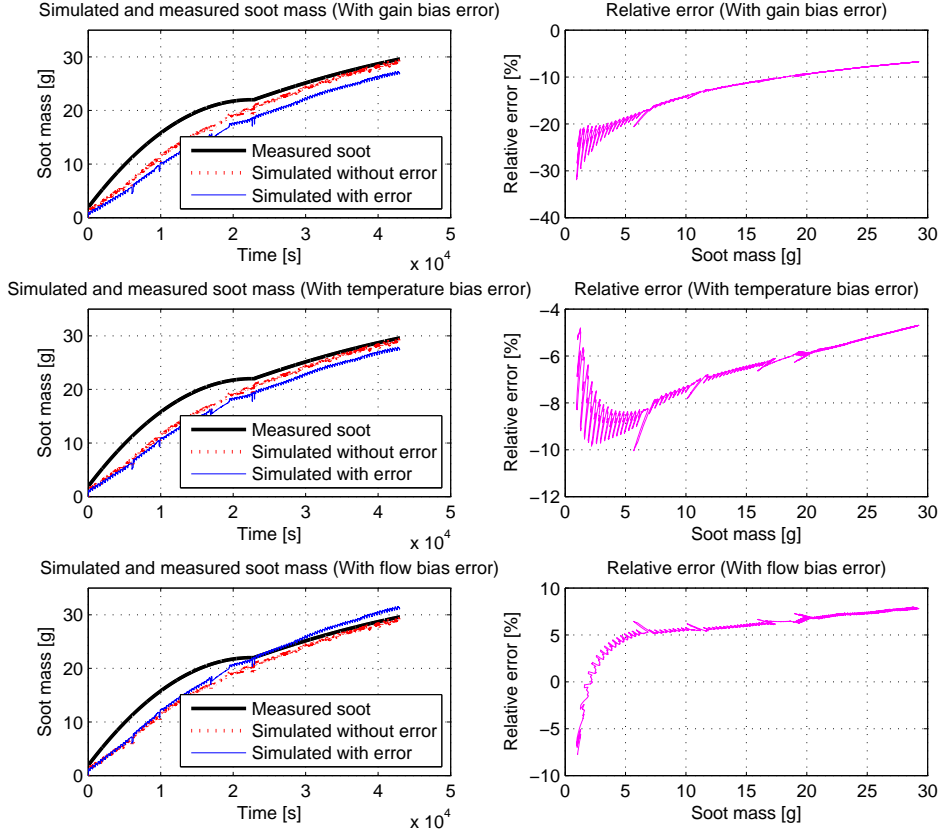
Figure A.4. The effect on the OE model with a bias error of 2 dB on the gain, 20 °C on the temperature and 20 m^3/h on the flow input signals, one at a time. Each row corresponds to a bias error for gain, temp and flow respectively. The left column is prediction with and without error compared to the weighted mass. The right column is the relative error for the prediction with the bias error compared to the prediction without error. The relative error decreases with increased soot mass for bias errors in gain and temperature but increases for a bias error in the flow.
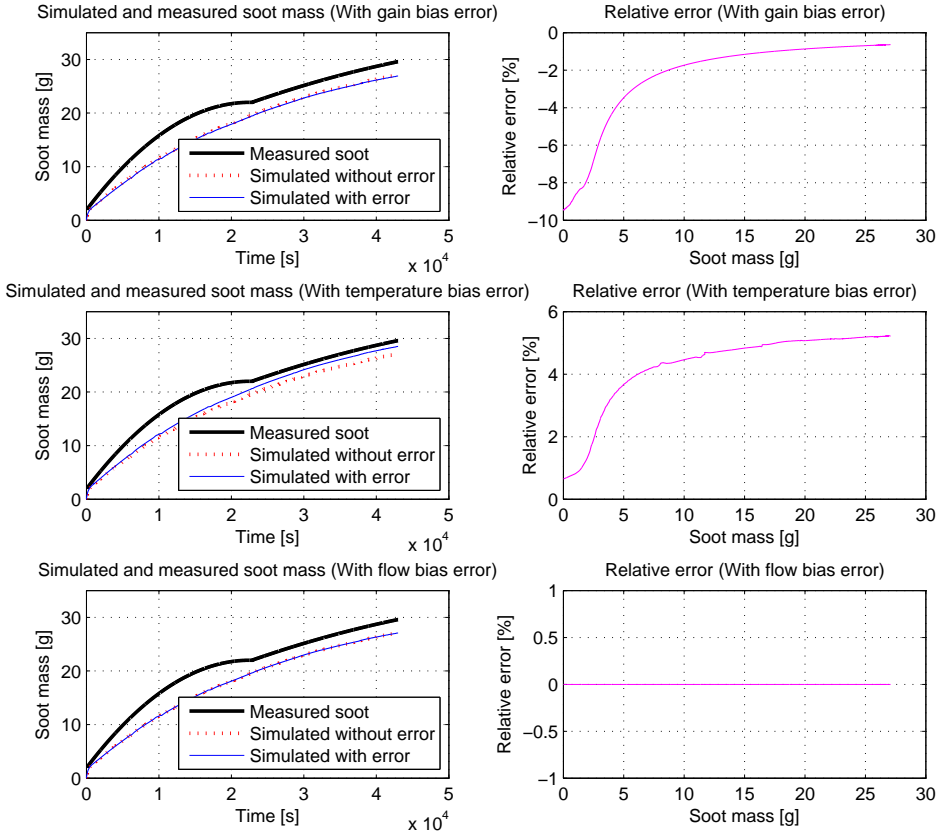
Figure A.5. The effect on the BJ model with a bias error of 2 dB on the gain, 20 °C on the temperature and 20 m^3/h on the flow input signals, one at a time. Each row corresponds to a bias error for gain, temp and flow respectively. The left column is prediction with and without error compared to the weighted mass. The right column is the relative error for the prediction with the bias error compared to the prediction without error. The relative error for a bias error in gain decreases towards zero with increased soot mass while a bias error in temperature stabilizes. Flow is excluded as an input signal to keep the model stable.
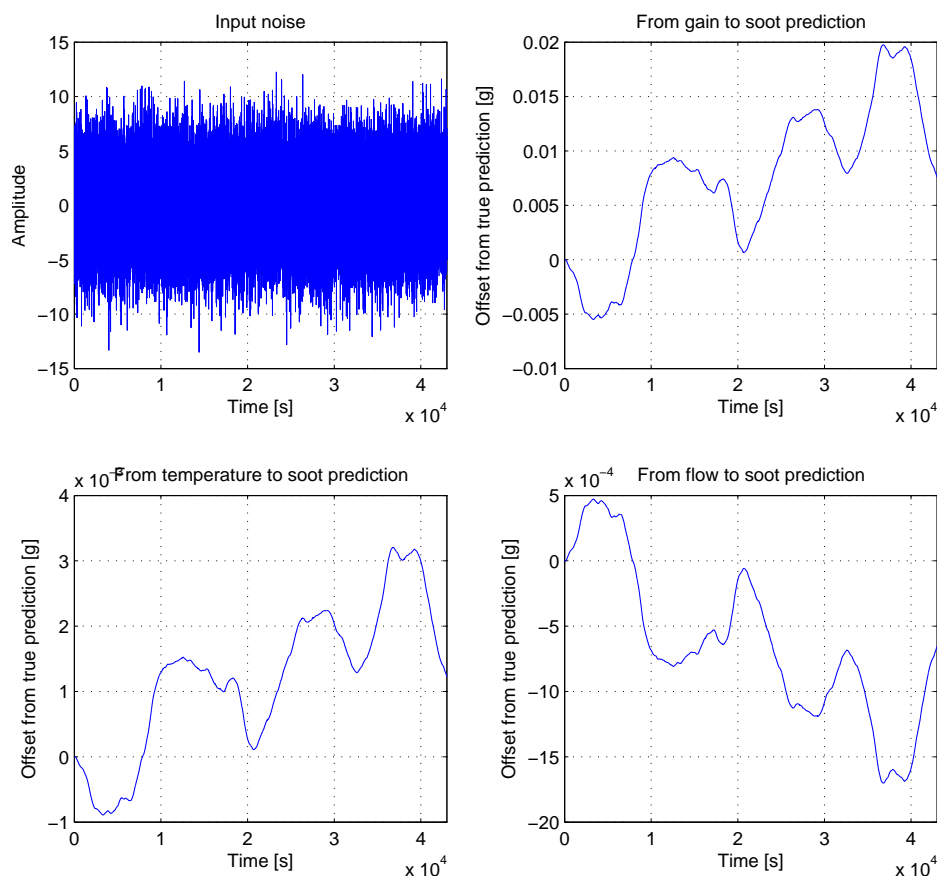
Figure A.6. The effect on the output for the ARX model when Gaussian noise, with mean value zero and variance 10, is added to each of the three input signals; gain, upstream temperature and flow, one at a time. In the figure the output from the simulation without noise is subtracted from the output from simulation with noise, thus only the output from the noise is shown. Top left: input noise, top right: noise added to the gain signal, bottom left: noise added to the temperature signal, bottom right: noise added to the flow signal.
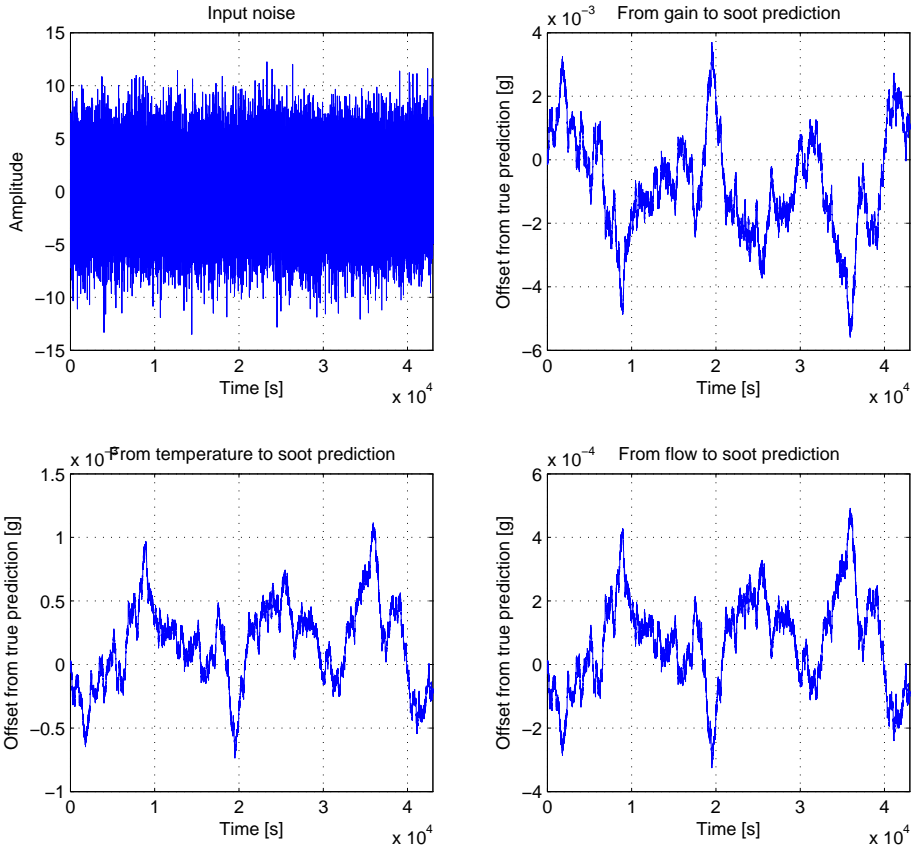
Figure A.7. The effect on the output for the reduced ARX model when Gaussian noise, with mean value zero and variance 10, is added to each of the three input signals; gain, upstream temperature and flow, one at a time. In the figure the output from the simulation without noise is subtracted from the output from simulation with noise, thus only the output from the noise is shown. Top left: input noise, top right: noise added to the gain signal, bottom left: noise added to the temperature signal, bottom right: noise added to the flow signal.

Figure A.8. The effect on the output for the ARMAX model when Gaussian noise, with mean value zero and variance 10, is added to each of the three input signals; gain, upstream temperature and flow, one at a time. In the figure the output from the simulation without noise is subtracted from the output from simulation with noise, thus only the output from the noise is shown. Top left: input noise, top right: noise added to the gain signal, bottom left: noise added to the temperature signal, bottom right: noise added to the flow signal.
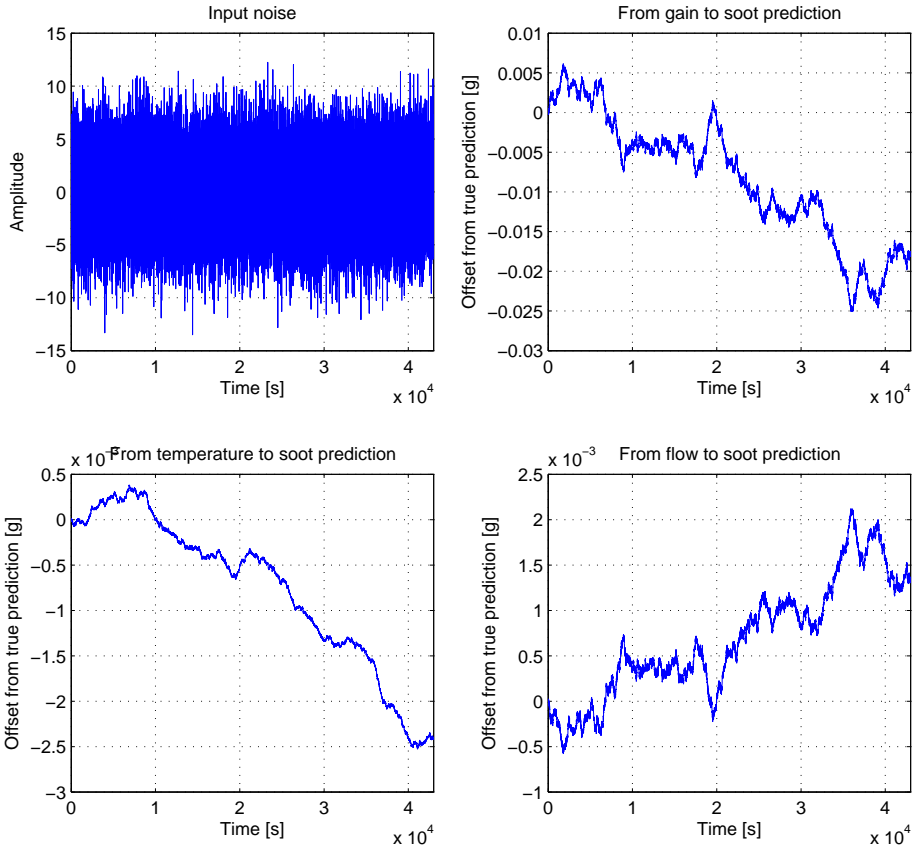
Figure A.9. The effect on the output for the OE model when Gaussian noise, with mean value zero and variance 10, is added to each of the three input signals; gain, upstream temperature and flow, one at a time. In the figure the output from the simulation without noise is subtracted from the output from simulation with noise, thus only the output from the noise is shown. Top left: input noise, top right: noise added to the gain signal, bottom left: noise added to the temperature signal, bottom right: noise added to the flow signal.
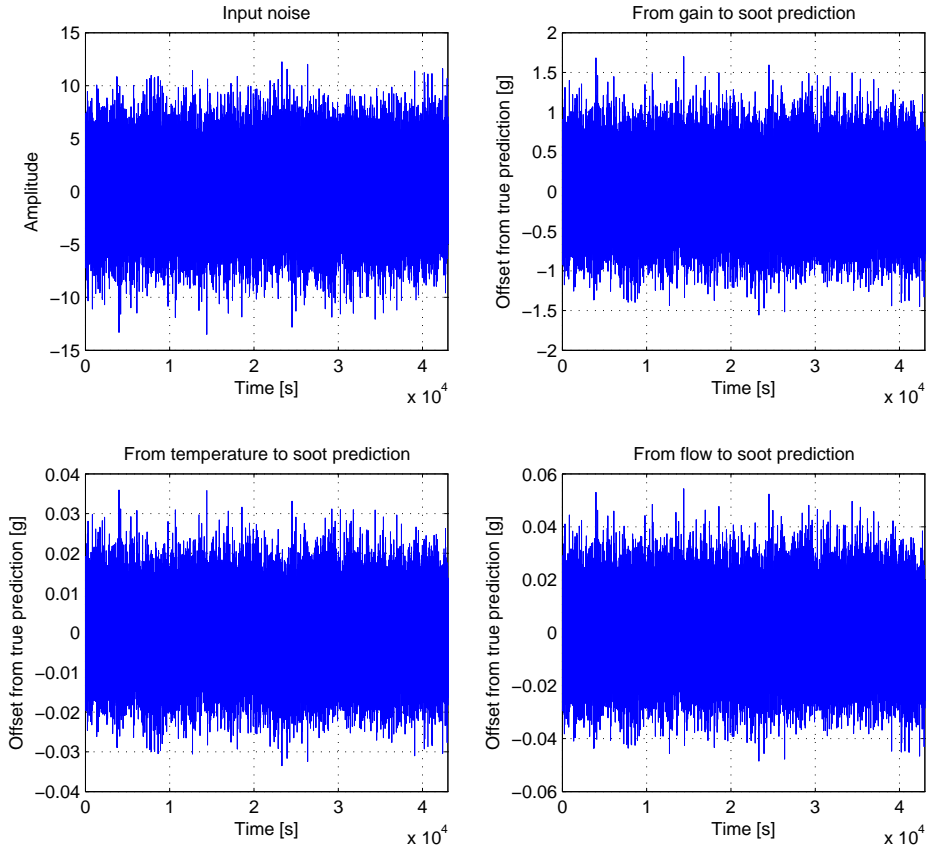
Figure A.10. The effect on the output for the BJ model when Gaussian noise, with mean value zero and variance 10, is added to each of the three input signals; gain, upstream temperature and flow, one at a time. In the figure the output from the simulation without noise is subtracted from the output from simulation with noise, thus only the output from the noise is shown. Top left: input noise, top right: noise added to the gain signal, bottom left: noise added to the temperature signal, bottom right: noise added to the flow signal.
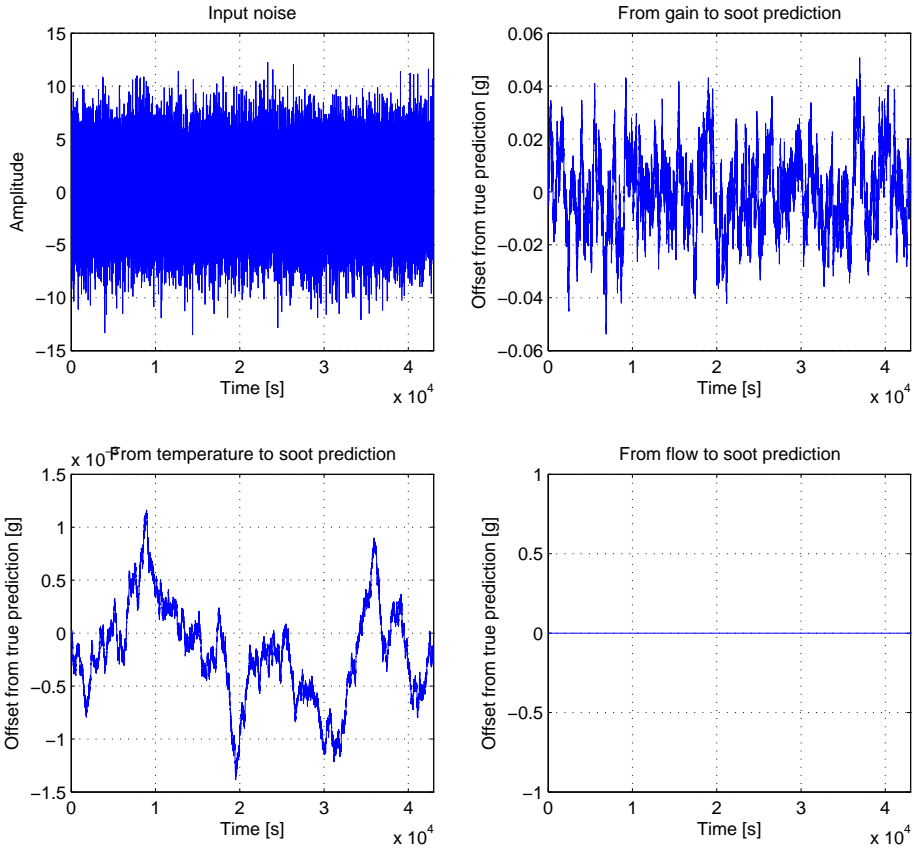
Bibliography

[1] Euro 5 and Euro 6 standards: reduction of pollutant emissions from light vehicles. `http://europa.eu/legislation_summaries/environment/air_pollution/l28186_en.htm`, Accessed 2012-02-06.

[2] Euro 5 techologies and cost for Light-Duty vehicles, TTNO report |05.OR.VM.032.1/NG|, October 2005. `http://ec.europa.eu/environment/air/pdf/euro_5.pdf`, Accessed 2012-02-06.

[3] Technical Strategy for Diesel Aftertreatment Systems, 2007. Volvo Confidential material.

[4] Initial RF characterization of a Volvo passanger car DPF, 2011. General Electric's initial evaluation.

[5] ACCUSOLVE Advanced Diesel Particulate Filter Soot Sensor, Performance Evaluation Guide, 2012. General Electric's manual.

[6] Matlab: System Identification Toolbox documentation, 2012. `http://www.mathworks.se/products/sysid/`, Accessed 2012-05-25.

[7] L. Andersson, A. Grennberg, T. Hedberg, R. Näslund, L. E. Persson, and B. von Sydow. *Linjär algebra med geometri.* Studentlitteratur, 1999. ISBN 9144009720.

[8] R. Bansal. *Handbook of engineering electromagnetics.* Marcel Dekker, 2004. ISB 9780824756284.

[9] P. J. Cunningham and P. H. Mackl. Measuring Particulate Load in a Diesel Particulate Filter. *SAE Technical Paper (2006-01-0868)*, 2006.

[10] T. T. Diller, M. J. Hall, and R. D. Matthews. Further Development of an Electronic Particulate Matter Sensor and Its Application to Diesel Engine Transients. *SAE Technical Paper (2008-01-1065)*, 2008.

[11] J. A. Dobrowolski. *Microwave Network Design Using the Scattering Matrix.* Artech House, 2010. ISBN 9781608071302.

[12] P. D. Eggenschwiler, D. Schreiber, and A. Liati. Active Regeneration Characteristics in Diesel Particulate Filters (DPFs). *SAE Technical Paper (2011-24-0185)*, 2011.

[13] G. Fischerauer, M. Förster, and R. Moos. Sensing the soot load in automotive diesel particulate filters by microwave methods. *IOP Science*, 2010. http://iopscience.iop.org/0957-0233/21/3/035108, Accessed 2012-02-01.

[14] G. Hagen, A. Piontkowski, A. Müller, D. Brüggemann, and R. Moos. Locally resolved in-situ detection of the soot loading in diesel particulate filters. *IEEE Sensors Conference 2011*, pages 1021–1023, Oct. 2011. http://ieeexplore.ieee.org/application/enterprise/entconfirmation.jsp?arnumber=6126979, Accessed 2012-02-01.

[15] A. Kondo, S. Yokoi, T. Sakurai, S. Nishikawa, T. Egami, M. Tokuda, and T. Sakuma. New Particulate Matter Sensor for On Board Diagnosis. *SAE Technical Paper (2011-01-0302)*, 2011.

[16] A. W. Kraszewski and S. O. Nelson. Microwave Resonator Technique for Moisture Content and Mass Determination in Single Soybean Seeds. *Instrumentation and Measurement, IEEE Transactions*, 43:791–796, 1994. http://ieeexplore.ieee.org/xpls/abs_all.jsp?arnumber=293475, Accessed 2012-02-01.

[17] L. Ljung. *System identification, theory for the user*. Prentice-Hall, 1987. ISBN 0138816409.

[18] L. Ljung. *Modellbygge och simulering*. Studentlitteratur, 2004. ISBN 9144024436.

[19] T. Ochs, H. Schittenhelm, A. Genssle, and B. Kamp. Particulate Matter Sensor for On Board Diagnostics (OBD) of Diesel Particulate Filters (DPF). *SAE Technical Paper (2010-01-0307)*, 2010.

[20] M. Ranalli, J. Klement, M. Hoehnen, and R. Rosenberger. Soot Distribution in DPF Systems. A simple and Cost Effective Measurement Method for Series Development. *SAE Technical Paper (2004-01-1432)*, 2004.

[21] S. Reiß, G. Fischerauer, and R. Moos. Radio frequency-based determination of the oxygen loading of automotive three-way catalysts. *AMA SENSOR + TEST Conferenses 2011 - SENSOR Proceedings, D4. - Gas sensors II*, pages 574–577, 2011. http://www.ama-science.org/home/details/505, Accessed 2012-02-01.

[22] S. Reiß, R. Moos, M. Wedermann, M. Spörl, A. Nerowski, and G. Fischerauer. RF-probing of Automotive Catalysts. *AMA SENSOR + TEST Conferences 2009 - SENSOR Proceedings II, B7. - Gas and Humidity*, pages 113–116, 2009. http://www.ama-science.org/home/details/216, Accessed 2012-02-01.

[23] S. Reiß, D. Schönauer, G. Hagen, G. Fischerauer, and R. Moos. Monitoring the Ammonia Loading of Zeolite-Based Ammonia SCR Catalysts by a Microwave Method. *Chemical Engineering Technology 2011*, 34:791–796, 2011. http://onlinelibrary.wiley.com/doi/10.1002/ceat.201000546/abstract, Accessed 2012-02-01.

[24] A. Sappok, L. Bromberg, J. E. Parks, and V. Prikhodko. Loading and Regeneration Analysis of a Diesel Particulate Filter with a Radio Frequency-Based Sensor. *SAE Technical Paper (2010-01-2126)*, 2010.

[25] M. Stumpf, A. Velji, U. Spicher, B. Jungfleisch, R. Suntz, and H. Bockhorn. Investigation on Soot Emission Behavior of A Common-Rail Diesel Engine during Steady and Non-Steady Operating Conditions by Means of Several Measuring Techniques. *SAE Technical Paper (2005-01-2154)*, 2005.

[26] R. Tibshirani. Regression Shrinkage and Selection via the Lassos. 1995. http://www.jstor.org/discover/10.2307/2346178?uid=3738984&uid=2&uid=4&sid=56113207443, Accessed 2012-04-27.

[27] C. S. Yoon, S. H. Song, and K. M. Chun. Measurement of Soot Mass and Pressure Drop Using a Single Channel DPF to Determine Soot Permeability and Density in the Wall Flow Filter. *SAE Technical Paper (2007-01-0311)*, 2007.

[28] N. Zhi, Z. Xinyun, and Y. He. Radio-Frequency (RF) Technology for Filter Microwave Regeneration System. *SAE Technical Paper (2000-01-2845)*, 2000.